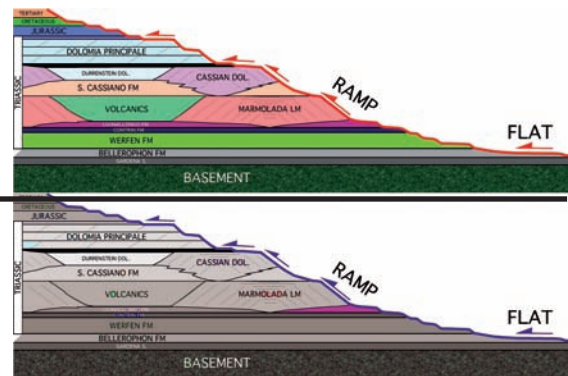


8. Tectonics and Sedimentation



Relationships among extensional tectonics, stratigraphy and inversion.

The interactions between tectonics and stratigraphy are schematically two-folds: 1) the effects of tectonics on the control of depositional sequences; 2) the control of paleotectonics and depositional sequences on the location of subsequent deformation.

Stratigraphy is mainly controlled by the combination of tectonics and eustatism. Oversimplified models considering only pure tectonic or eustatic control on stratigraphy are misleading. Their relative importance has to be taken into account considering the magnitude and origin of the different orders of eustatic oscillations and their association with the tectonically controlled vertical motions occurring in the various geodynamic and tectonic scenarios in which they operate. For example, along passive margins the interference between tectonics and eustatism is different during rifting and drifting stages. During rifting tectonic subsidence prevails, whereas thermal subsidence is more important during drifting. Therefore, as in contractional environments, also in extensional settings the interference

between tectonics and eustatism varies as a function of how, where (kind of geodynamic environment) and when (one of the various stages of third order cycles that develop during sea-level rises or falls of second cycle) it occurs. An important relationship between tectonics and stratigraphy can be observed in extensional or transpressional growth faults. If subsidence rate is slower than the velocity of the environment to re-equilibrate and maintain the same facies along the fault, then subsidence across the fault plane will control only the sedimentary thickness at the two sides of the fault, since sedimentation will manage to level continuously the structural step. However, when the velocity of the fault is faster than sedimentation rates, the fault will produce a morphological step and will control both facies changes and sedimentary thickness variations between hangingwall and footwall. In this second case, local depositional sequences, not globally correlatable, can develop: debris flows associated to fault escarpment or to rollover anticline flanks cannot be considered as low-stand wedges.

The aggradation of a carbonate platform is controlled by subsidence and carbonate pro-

duction. The platform break of a carbonate platform is therefore direct function of the subsidence rates of an area. In the Dolomites, for example, coeval carbonate platforms show different shapes of the platform break surface. This is due to the fact that such platforms grew in areas characterised by different subsidence rates generated by the Triassic transtensional tectonics. A strong and fast subsidence generates a subvertical platform break surface, whereas a subhorizontal platform break surface is generated during phases of low or null subsidence.

A frequently disregarded parameter is the subsidence component related to compaction of the sedimentary cover. The more the sediment succession is heterogeneous, the more compaction is irregular: this can produce depositional sequences confined to restricted basins controlled by differential compaction.

The three dimensional reconstruction of inversion structures remains an open problem.

Generally, inversion is considered in two dimensions (e.g., a graben inverted to produce a pop-up). However, the direction of compression can vary widely with respect to the preceding extension. In the Southern Alps, for example, alpine compression ($N0^{\circ}-30^{\circ}W$) is oblique to Mesozoic extensional paleostructures (i.e., extensional growth faults oriented $N10^{\circ}E-N10^{\circ}W$) (fig. 148). Extensional paleofaults dipping to the east were easily cut and transported passively along thrust faults, whereas those dipping to the west were easily re-sheared as sinistral transpressional faults. As already mentioned, inversion (or re-shear) of a fault occurs when peculiar conditions are respected (e.g., low angle both for strike and dip between the thrust fault and the pre-existing normal fault; high fluid pressure). The shortening of a platform-basin system can produce different interference geometries for different directions of compression relative to the direction of the platform margin. The concept

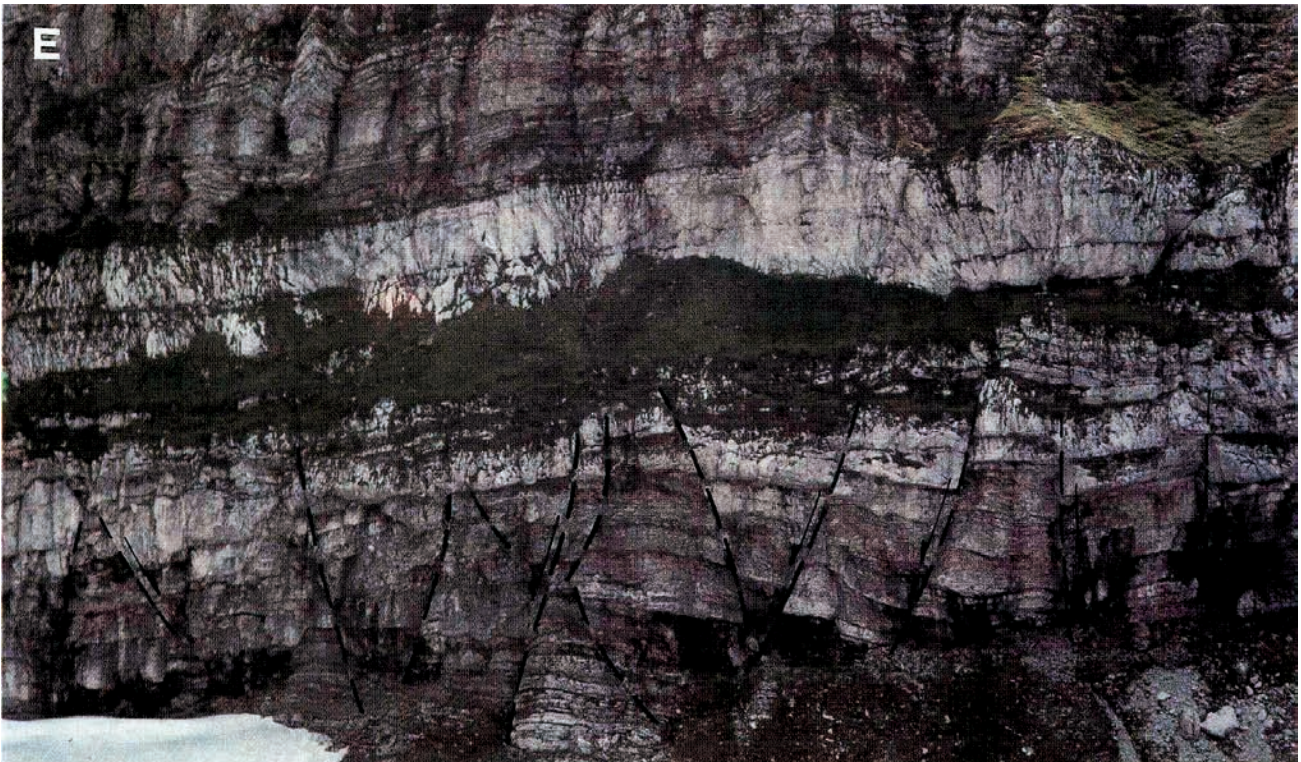


Fig. 148 - System of grabens with N-S direction in Dogger sediments (synchronous to the deposition of the Fonzaso and Calcare del Vajont Fms.) cropping out along the northern flank of Mt. Mangart (area of Tarvisio). It can be considered as a field example of the Mesozoic Southalpine extensional tectonics.

of platform should however be split in two concepts: structural platform (that is generally retrograde since extensional tectonics migrates and induces a margin retrogression) and sedimentary platform (that is generally prograde due to the advancement of a carbonate platform or of a delta).

The front of a fold-and-thrust belt is generally of three types: 1) triangle zone; 2) fault propagation fold; 3) fault bend fold. A syn-sedimentary fault in the upper crust of a certain region represents a strong anisotropy due to the different thickness of lithologies in hanging-wall and footwall. Differences in the embrication structural style can be frequently observed at the two sides of the fault: for example, an imbricate fan on one side and a pop-up on the other side. In nature the three above mentioned front geometries may develop separately or may be combined and coexist. Rheology controls and determines the predominance of one of the three mechanisms on the others. For example, triangle zones are best developed in basin sedimentary successions, rich in shales and therefore more prone to flexural slip. The activation of flexural slip processes is also necessary in fault-propagation folds. Fault-propagation folds and fault-bend folds can coexist in the same structure both in section and along strike. For example, the propagation of a fault at the hinge of a fold may occur with a ramp-and-flat trajectory, so that the two folding mechanisms may be superimposed.

Some examples from the Southern Alps (interactions among Mesozoic extensional tectonics, stratigraphy and Alpine shortening)

The Southern Alps are a regional example for some general considerations on the relationships among extensional tectonics, lithological and facies variations (both horizontal and vertical) and alpine inversion (both Southalpine and Dinaric) (figs. 149 - 163).

The irregular rheology of the Southern Alps sedimentary cover is evident observing the

ramp and flat trajectories of the thrust surfaces. It can be commonly observed that sequence boundaries or maximum flooding surfaces acted as preferential decollement levels. Obviously evaporitic and shaly levels or horizons characterised by strong lithological contrasts constitute major detachment surfaces. The main detachment levels are: Bellerophon Fm (Upper Permian) and Werfen Fm (Scythian) in the Dolomites, together with the pelagic deposits of the Livinallongo Fm (Ladinian) and San Cassiano Fm (Carnian). In the Venetian Prealps, the major decollements are concentrated in the Cretaceous pelagic deposits (Biancone and Scaglia Rossa Fms.) and in the flyschoid deposits of Paleocene-Eocene age. Ramp geometries of thrust faults are frequent at the margins of carbonate platforms and along clinostratifications. The horsts are often located along frontal, oblique or lateral ramps, as a function of their geometry with respect to the direction of maximum compression.

Some paleostructures can be identified by structural undulations in the thrust belt. Such undulations occur frequently above inherited normal syn-sedimentary faults or in correspondence with facies and thickness variations. Several physical parameters affect the final structure of the belt. In particular, a strong influence is exerted by the orientation of shortening with respect to pre-existing extensional faults and by the facies involved. For example, high angle normal faults dipping in a direction opposite to that of the thrust surfaces are seldom reactivated, whereas normal faults dipping to the same direction or at low angle to the thrust surface are more easily inverted as transpressional or reverse faults. Normal faults or facies limits oriented perpendicularly to subsequent thrusts are often loci of structural undulations in the belt or of transfer zones.

From the structural analysis of the Southalpine belt it is evident that each structural undulation is controlled by pre-existing

rheological anisotropies (variations of thickness and facies, inherited faults, etc.). Consequently we may hypothesize the occurrence of paleostructures, even where these are undiscovered, on the basis of the occurrence of structural undulations within the belt. The largest structural undulation of the Southern Alps occurs along the Giudicarie fault lineament, which is most probably one of the largest Mesozoic crustal anisotropies between the Trento Platform to the east and the Lombard Basin to the west. Towards the east, further first order structural undulations occur at the transitions between Trento Platform and Belluno Basin and between Belluno Basin and Friuli Platform, which are the more significant structural features of the area. Various second order undulations occur in correspondence with the minor paleostructures at the margins or within the above mentioned major structural domains, which were unstable features through time. As analogously observed in seismic lines at the margins of present-day plate margins, such domains were progressively cut by extensional and transfer faults that dissected the structural highs and were active at different places in different times. For example, the eastern margin of the Trento Platform retrogressed, from a structural point of view, to the west from the Jurassic to the Cretaceous. This controlled the thickness and sometimes the facies of sediments. The differences on the two sides of the Mesozoic extensional fault system separating the Friuli Platform and the Belluno Basin controlled the geometry of the front of the Venetian Southern Alps front. To the west, within the Belluno Basin, the front is accommodated by a triangle zone (Bassano Line) and the foredeep clastic sediments are folded and tilted to the south, whereas to the east the frontal thrust front crops out along the Maniago Line and the clastic foredeep sediments are overthrust.

The structural undulations at the front of the belt also control the syn-tectonic clastic depo-

sition in the foreland basin. The onlaps on the growing flank of the frontal fold of the belt occur unconformably only along dip if the fold is cylindrical (i.e., without axial undulations). On the contrary, the unconformity will occur both along dip and strike in non-cylindrical folds (i.e., along deep anisotropies inherited by compressional tectonics).

Interactions between tectonics, eustasy, compaction and sedimentation.

In general, thrust fault activation migrates towards the foreland in fold-and-thrust belts. Consequently, also syntectonic clastic deposits migrate towards the foreland. In several works, the evolution of fold-and-thrust belts is described in terms of orogenic phases or pulses. This may suggest misleadingly that shortening is limited to periods separated by quiescence stages. It is here stressed that the shortening in contractional belts is rather constant through time and follows the rate of plate motions that is rather regular, as indicated by the spreading rates at middle-oceanic ridges. Such continuous shortening is accomplished by the growth of folds related to fault-propagation and fault-bending. These folds generate episodic and local uplifts within a belt that constantly migrates towards the foreland. However, such local events may not be interpreted as the evidence of a phase-like evolution of shortening in fold-and-thrust belts (figs. 164, 165).

For example, a single fold with a 1-3 km amplitude can develop in a time span variable between 0.5 and 5 Ma. During the growth of an anticline (either sub-aerial or marine) the clastic sedimentation drapes and onlaps the uplifting zone.

The anticlines are eroded and represent the source area for the foredeep deposits. The growth of an anticline may occur during a part of a third order cycle (e.g., low stand, transgressive, high stand) and consequently sedimentation may be controlled by the interplay

between uplift rates and eustatic fluctuations. Such a combination may be highly variable and random. The uplift rates of an anticline may in general be considered constant through time, but may also be irregular, especially in transpressional settings.

During a low stand, the uplift rates of the anticline and the rates of eustatic fall need to be summed up. This time interval obviously will register the largest relative sea-level fall and the period will be characterised by strong erosion of the anticline. During a transgression stage, the effects of tectonic uplift may be in part or

totally compensated by the eustatic rise. As a result the relative sea-level may remain approximately constant along the flanks of a growth anticline and erosion may be minimal. The subsequent high stand represents an intermediate situation, in which the structural uplift is only in part (or not at all) compensated by the eustatic rise. Consequently also erosion is intermediate between that occurring in low stand and transgressive phases. Therefore, each fold has its own tectonic and eustatic history. The resulting syntectonic stratigraphy is therefore highly dependent on when, where and

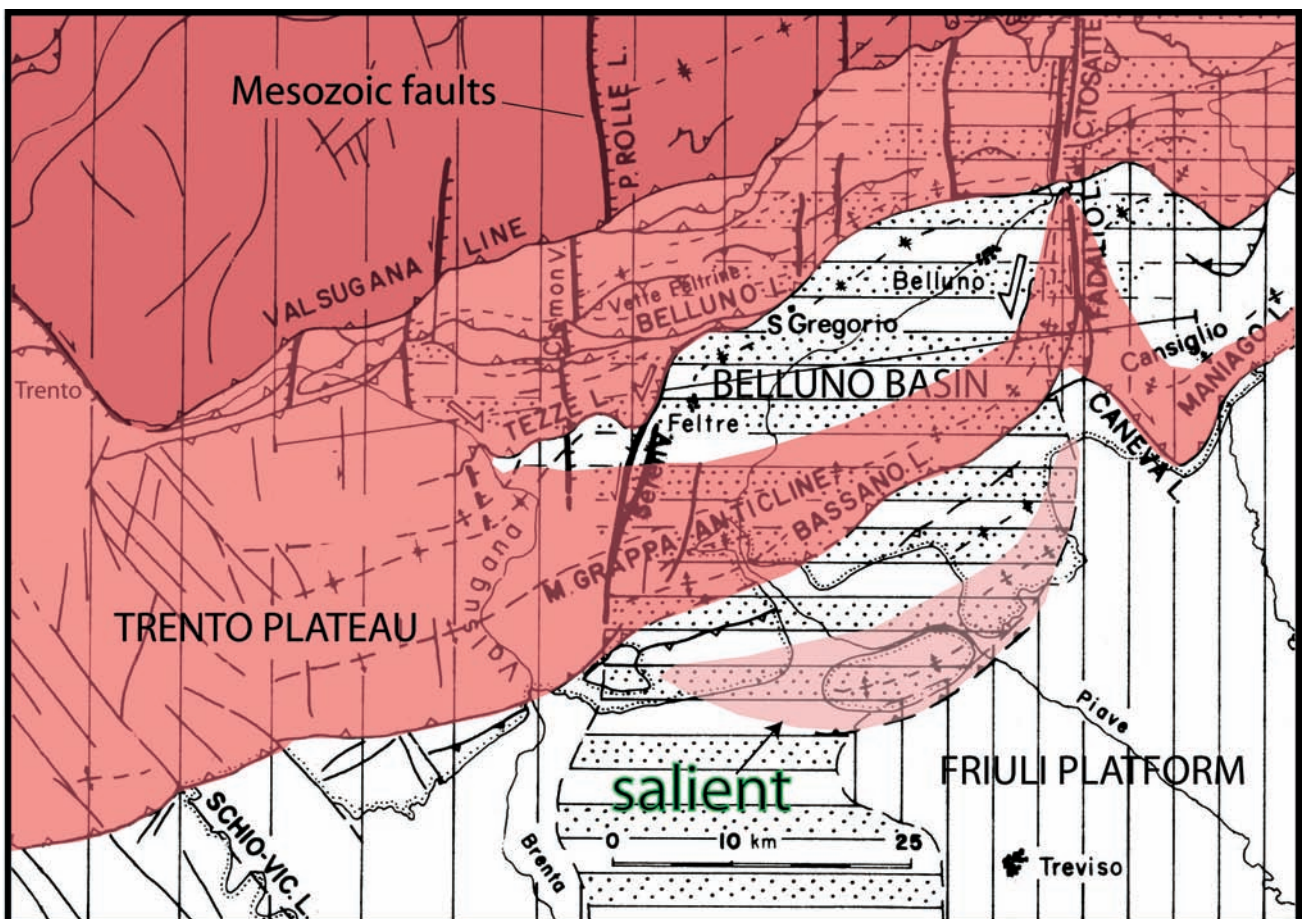


Fig. 149 - The Mesozoic horts and grabens and facies transitions controlled the geometry of the Venetian Alps fold-and-thrust belt, producing undulations of the structures that are characterised by non-cylindrical shape. Transpressional fault systems and transfer faults are localised along inherited Mesozoic extensional faults and along thickness and facies variations of the sedimentary cover. The shaded pink zone represents the morphological and structural relief of the area. The darker colors are toward the more internal thrust sheets. Note that such a relief diminishes rapidly from the Trento Platform towards the east where compressional tectonics affected the sediments of the Belluno Basin. At the eastern margin of the basin, a major sinistral transpressional zone occurs at the intersection with the Friuli carbonate platform. The structural relief is lower but more diffuse within the Belluno Basin which is richer in shaly content, allowing lower friction in the decollement zones, and forming a salient of the thrust belt front (after DOGLIONI, 1992). In the salient, ramp distance is wider and the topography is lower.

how the fold develops. A fold is therefore a local process that represents only a spatial and temporal element of a mountain belt that needs to be studied in all its aspects. Dating a fold, filtering the effects of the eustatic oscillations, means deciphering one single step of the complex evolution of a belt.

A crucial point in the study of mountain belts is the dating of the deformation phases. The stratigraphic chronologies, based on transgressive conglomerates may however be misleading. For example, in the Venetian Southern Alps a strong Messinian deformation phase, characterised by strong conglomeratic sedimentation (Montello and Pontico Conglomerates), has been proposed for a long time. However, the eustatic curve shows a sharp global low stand phase during the Messinian.

It may be thus alternatively proposed that the Venetian Southern Alps developed quite regularly from the Oligocene and that the Messinian sea-level fall, even if restricted to the

Mediterranean, may have induced a strong erosional phase, non necessarily associated to a tectonic pulse.

The geometry of sediments onlapping normal fault escarpments or the flanks of anticlines, is normally considered to be controlled by the relationship between tectonics and sedimentation but it may be additionally controlled by differential sediment compaction. For example, in the Apennines the basal strata onlapping platform sediments along Mesozoic normal fault paleoescarpments commonly dip considerably (as much as 20°-30°) toward the basin when platform strata are retrodeformed to horizontal so to eliminate the geometrical effects of Tertiary compressional tectonics. These geometries are usually interpreted, in the field and in seismic lines, as the effects of normal drag along synsedimentary faults. Similarly, basinward dip affecting clastic sediments onlapping anticlines flanks in the Po Plain has been interpreted as the effect of synsedimentary growth of the anticline. Although

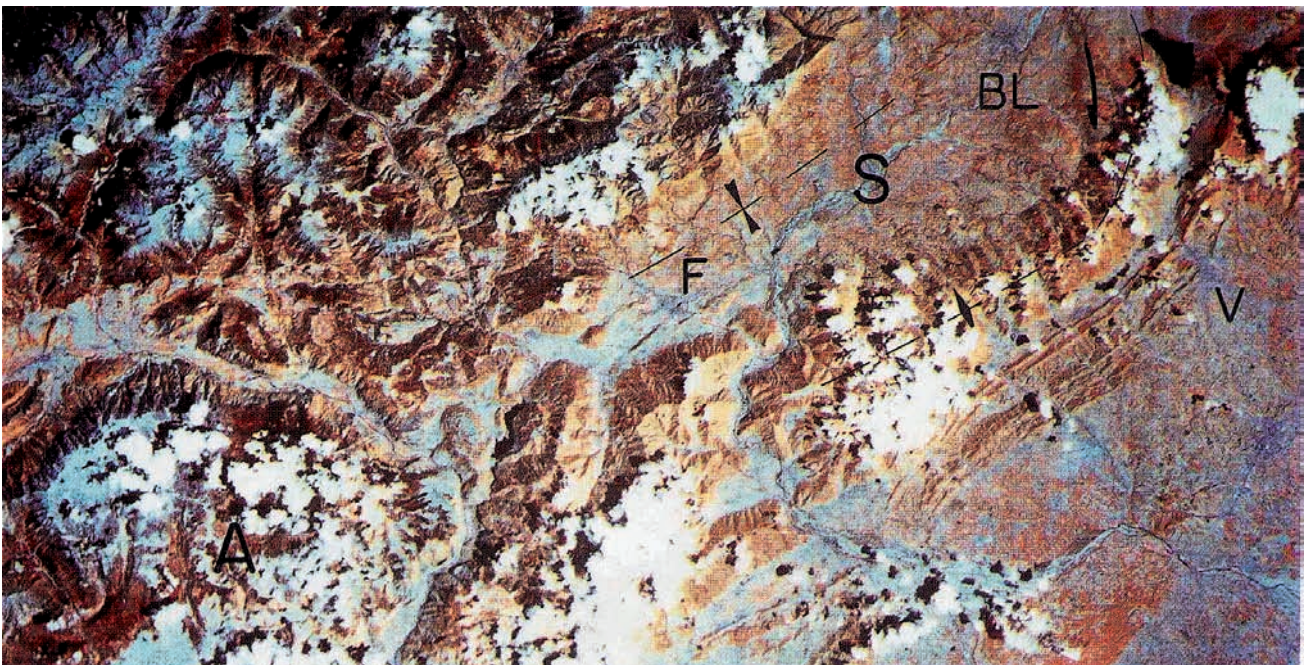


Fig. 150 - Satellite image of the Venetian Alps. Notice that the dimension of the morphological high of the Asiago Plateau (A), corresponding to the Mesozoic Trento Platform, drastically reduces to the east within the Belluno Basin, broadly correspondent with the Belluno syncline (S) located between Feltre (F) and Belluno (B). To the right the undulation of the Mt. Grappa-Visentin Anticline can be observed. This anticline developed in a transpressional system, at the intersection between the Belluno Basin and the Friuli Platform. V, Vittorio Veneto.

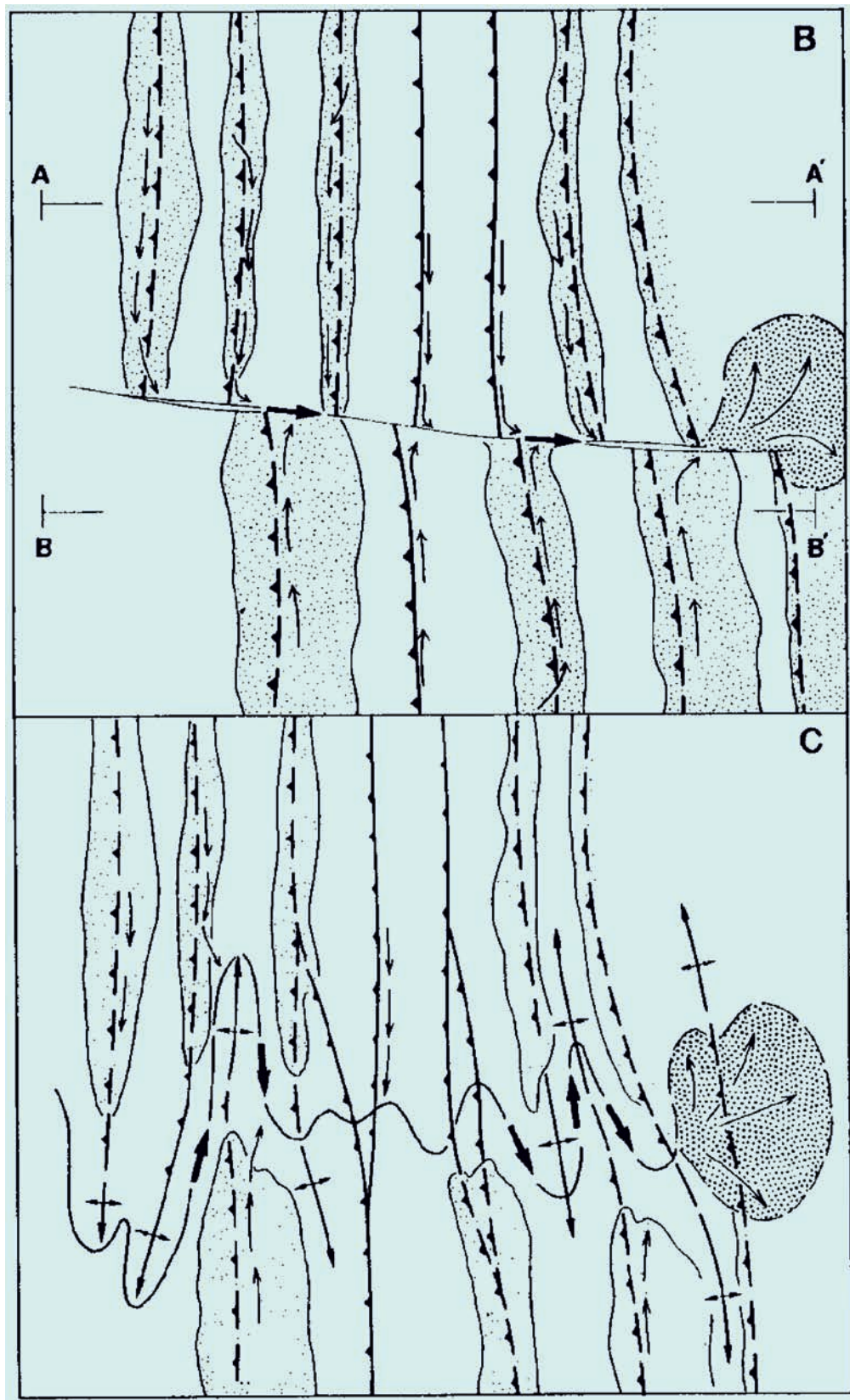


Fig. 151 - Structural undulations along strike, and transfer zones in general, control the hydrographic pattern. Therefore the coarser and larger accumulation of clastic material at the front of the thrust belts occurs more frequently where internally in the belt there are transfer zones (after LAWTON *et alii*, 1994).

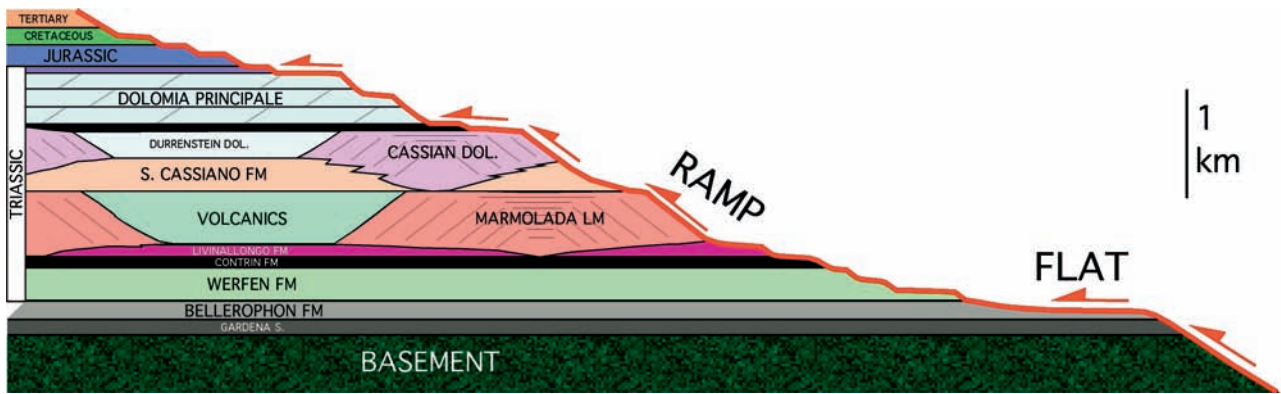


Fig. 152 - Potential control of the stratigraphic succession on the localization of ramps and flats (decollement surfaces) of thrust faults in the Dolomites region. The basement includes the Gardena Sandstone, the older Permian porphyrites and the underlying Hercynian crystalline basement. Notice the occurrence of margins of Ladinian and Carnian carbonate platforms (Marmolada Limestone and Cassian Dolomite respectively) that can be the loci of thrust ramps. The Bellerophon Fm (Upper Permian), consisting mainly of evaporitic sediments such as gypsum, shales and marls, is characterised by flat geometries of thrust faults, similarly to other relatively less competent formations (e.g., Andraz Horizon of the Werfen Fm and Raibl Fm).

the feasibility of such an interpretation is not neglected, the results of numerical simulations of sedimentation demonstrate that the dips observed in the field or in seismic lines can also (or in part) be explained by differential compaction (SKUCE, 1994; CARMINATI & SANTANTONIO, 2005; SCROCCA *et alii*, 2007). The role of differential compaction is supported by numerical modeling (figs. 166, 167).

The evolution of the belt will be therefore registered by punctual information provided by the unconformities. The dip of the basement monocline varies between 0° and 5° in belts associated to subductions that follow the flow of the mantle (i.e., directed to the E-NE), and between 5° and 10° in the belts associated to subductions contrasting the mantle flow (i.e., directed to the W). In this latter case, cha-

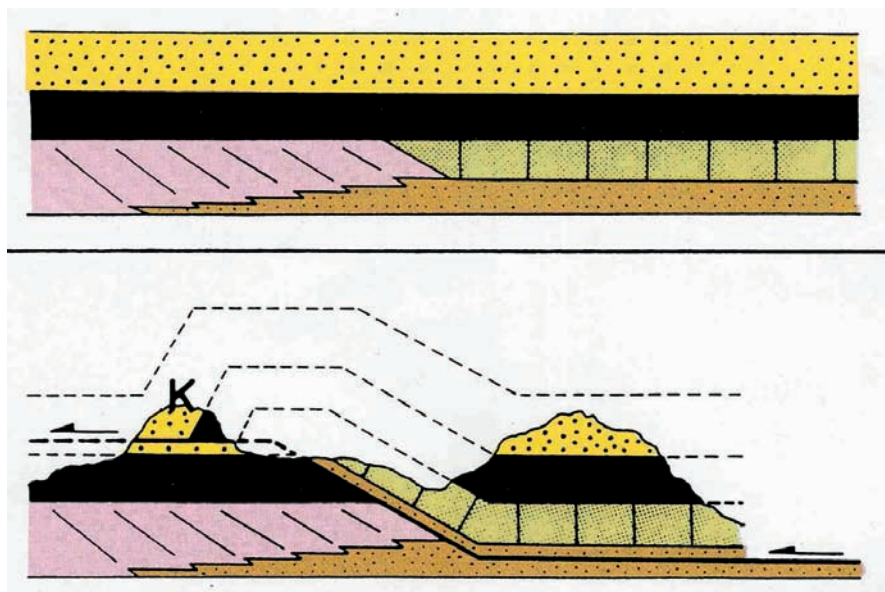


Fig. 153 - Schematic section of a carbonate platform (violet) and of the adjacent basin covered and levelled by later sediments. The margin of the platform becomes the area where compressional stresses are focussed. For this reason, the chance that ramp geometries of the thrust faults may form in this inherited structure is rather high. The klippen (K) of the Dolomites are interpreted as remaining parts of the hanging-wall of thrust faults similar to that shown in this figure.

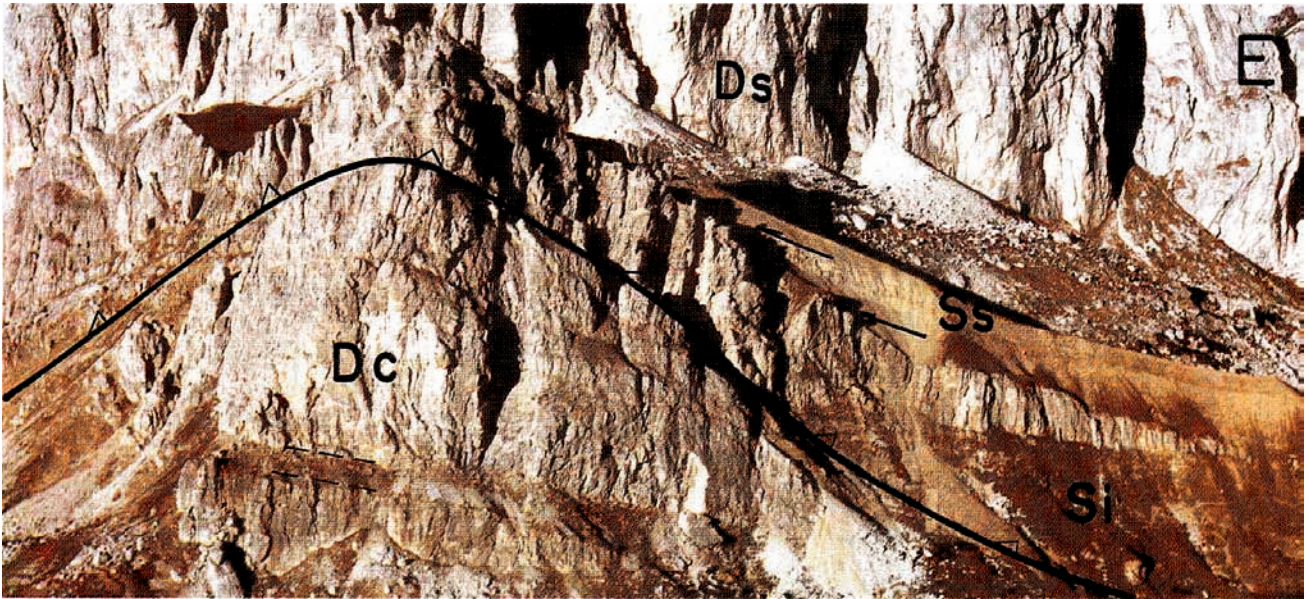


Fig. 154 - The Sasso di Richthofen (central Dolomites) is a prograding edge of the Lower Cassian Dolomite (lower Carnian, D1) that was doubled by a thrust that partially used as a ramp the clinostatification of the megabreccias. Notice within the San Cassiano Fm the thinning of the body of megabreccias towards the right that onlaps the same body. D2, Upper Cassian Dolomite; S1, Lower San Cassiano Fm; S2, Upper San Cassiano Fm.



Fig. 155 - Northern wall of the Croda del Vallon Bianco (Ampezzo Dolomites), consisting of Liassic Calcari Grigi in which a W-verging thrust cuts a pre-existing extensional fault of Upper Jurassic - Lower Cretaceous? age.



Fig. 156 - WSW-verging thrust of the Remeda Rossa in the Ampezzo Plateau. The thrust surface is sub-horizontal, the hanging-wall consisting of folded and partly overturned Calcarei Grigi (G) and the footwall consisting of Cretaceous marls (K; in the meadows), extremely deformed by the shear zone.



Fig. 157 - Detail of the previous figure. In the hanging-wall of the Remeda Rossa thrust the Calcarei Grigi sediments are overturned along the broken flank of a fault-propagation fold. In these sediments, a shear zone can be observed. If the sediments are retro-deformed to the pre-overturning position, the shear zone is interpretable as a syn-sedimentary extensional fault. Notice that the fault is sutured at the bottom of the picture. It may, however, be argued that the flexural slip necessary to accommodate the fold formation may have obliterated such an inherited shear zone. In this case the shear zone could be interpreted as an antithetic Riedel fault of the main thrust plane.

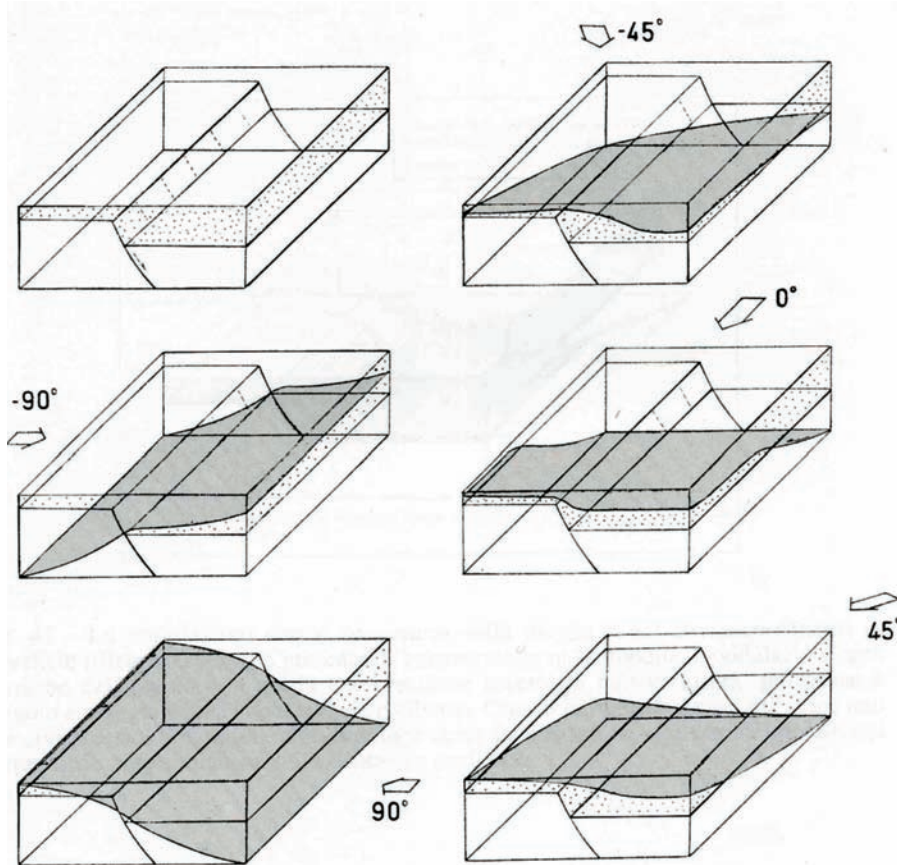


Fig. 158 - During inversion stages, a given normal syn-sedimentary fault can be shortened with very variable angles. The fault-hinge zone represents a strong anisotropy within the shortened body and compressional stresses may easily focus around the extensional lineament. The stress field in the vicinity of the fault is, however, controlled also by the angle between the principal stresses directions and the inherited geometry (both strike and dip) and by the rheology of the rocks constituting both hanging-wall and foot-wall. The entity of inversion is surely influenced by the direction of compression with respect to the attitude of the paleostructure. Lateral ramps frequently develop in the areas of inherited fault hinge. A compression oriented at -90° to the strike of the paleostructure may cut the paleostructure without producing appreciable inversion along the old extensional lineament, with the exception of minor backthrusting. The more significant inversions develop when the extensional paleofaults dip to the same direction of the thrust fault planes and the angle between the shortening direction and the dip direction of the extensional fault is small. For example, in the Southalpine belt, the Mesozoic extensional faults striking about N-S and dipping to the east were cut and involved in the alpine folding without significant deformation. In other words they are much more preserved and recognizable than Mesozoic normal faults with the same strike but dipping to the west that were frequently reactivated as sinistral transpressional faults.

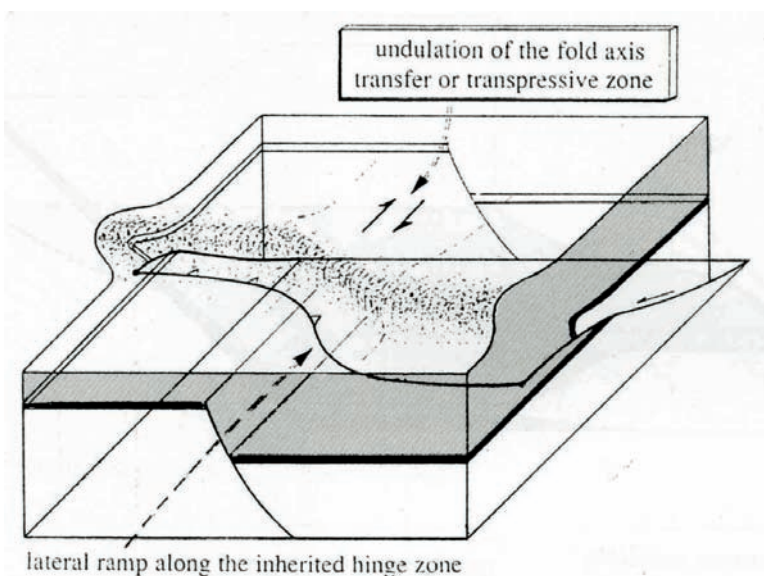


Fig. 159 - Undulations of fold axis and thrust plane reflect the presence of paleostructures (i.e. normal faults or facies changes) at depth. The undulation of the fault-propagation fold will be a function of the angle of compression with respect to the buried feature. The drawing represents the case of 0° , with compression parallel to the pre-existing normal fault strike. Lateral ramp forms along the inherited anisotropy. Between 0° and 30° - 40° , there are the strongest undulations as in the example of the next figure.

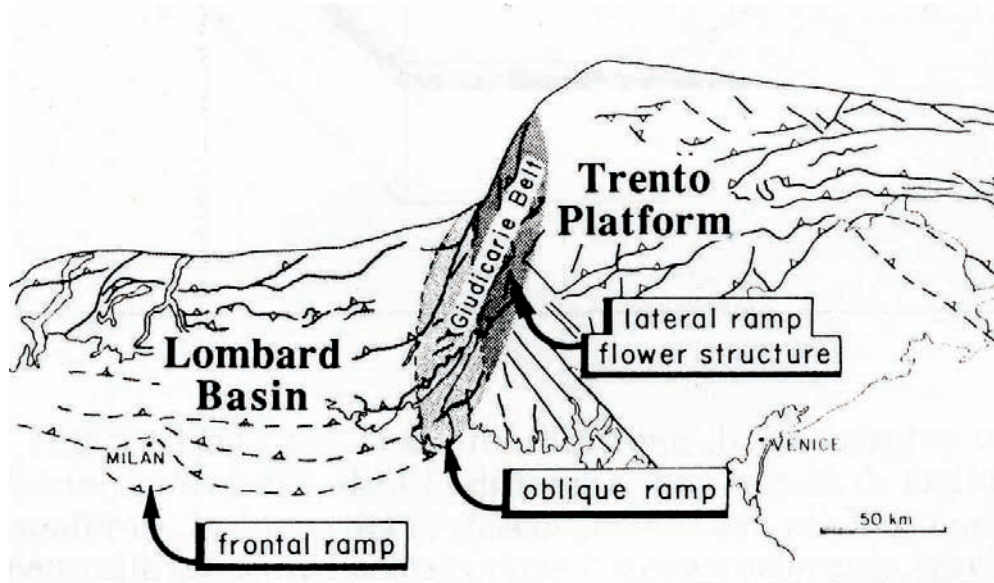


Fig. 160 - The sinistral transpression along the Giudicarie fault system represents the strongest structural undulation of the Alps and developed as a sinistral transpressional reactivation of a system of extensional faults dipping to the west (one of the major fault is the Ballino Line; CASTELLARIN, 1972). This undulation developed at the border between the Lombardian Basin to the west and the Trento Platform to the east (DOGLIONI & BOSELLINI, 1987).

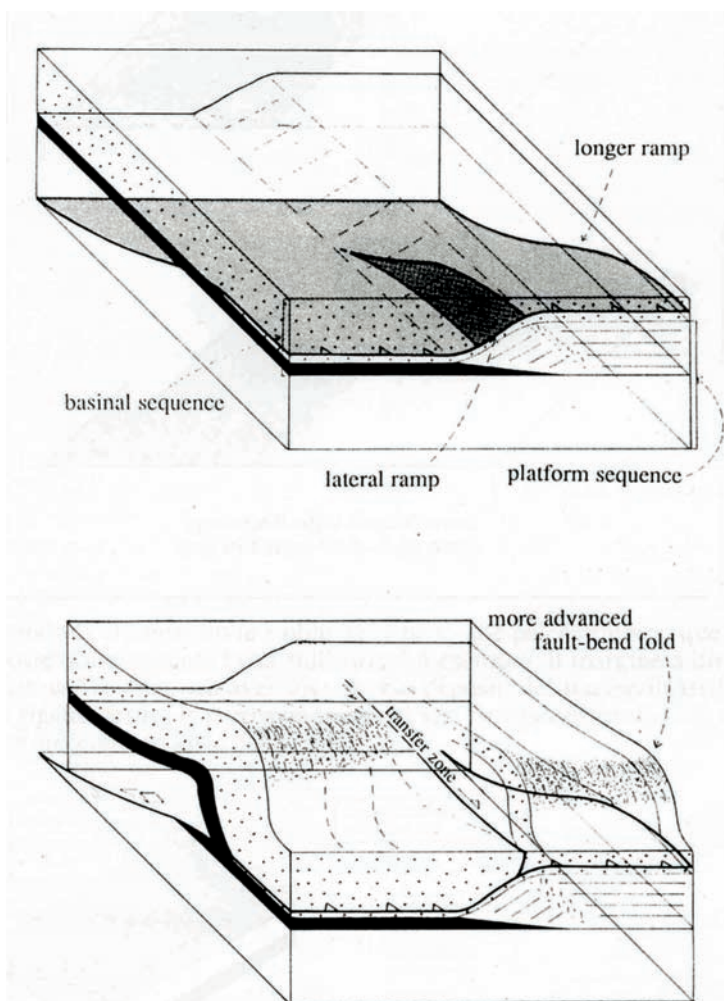


Fig. 161 - Example of shortening parallel to the margin between a carbonate platform and a basin. In this case the difference of ramp dips between basin and platform sediments will produce a longer thrust ramp in the platform sequence with respect to the basin sequence, where the thrust surface, propagating in less competent sediments, will tend to become horizontal. This will produce a more advanced anticline in the platform sequence with respect to that in the basin sequence, with a transfer lateral ramp connecting the two structures. This model could be applied to the western margin of the Friuli Platform, where the Cansiglio anticline developed in the platform sediments in the hanging-wall of the Maniago Line is more advanced than the Mt. Grappa-Visentin Anticline developed in the Belluno Basin. The two anticlines are connected by the Fadalto - Caneva transfer zone. It is, however, to be noticed that the Mt. Grappa-Visentin Anticline is not the front of the belt, which coincides with the more external Montello Anticline, within the salient in the Belluno Basin.

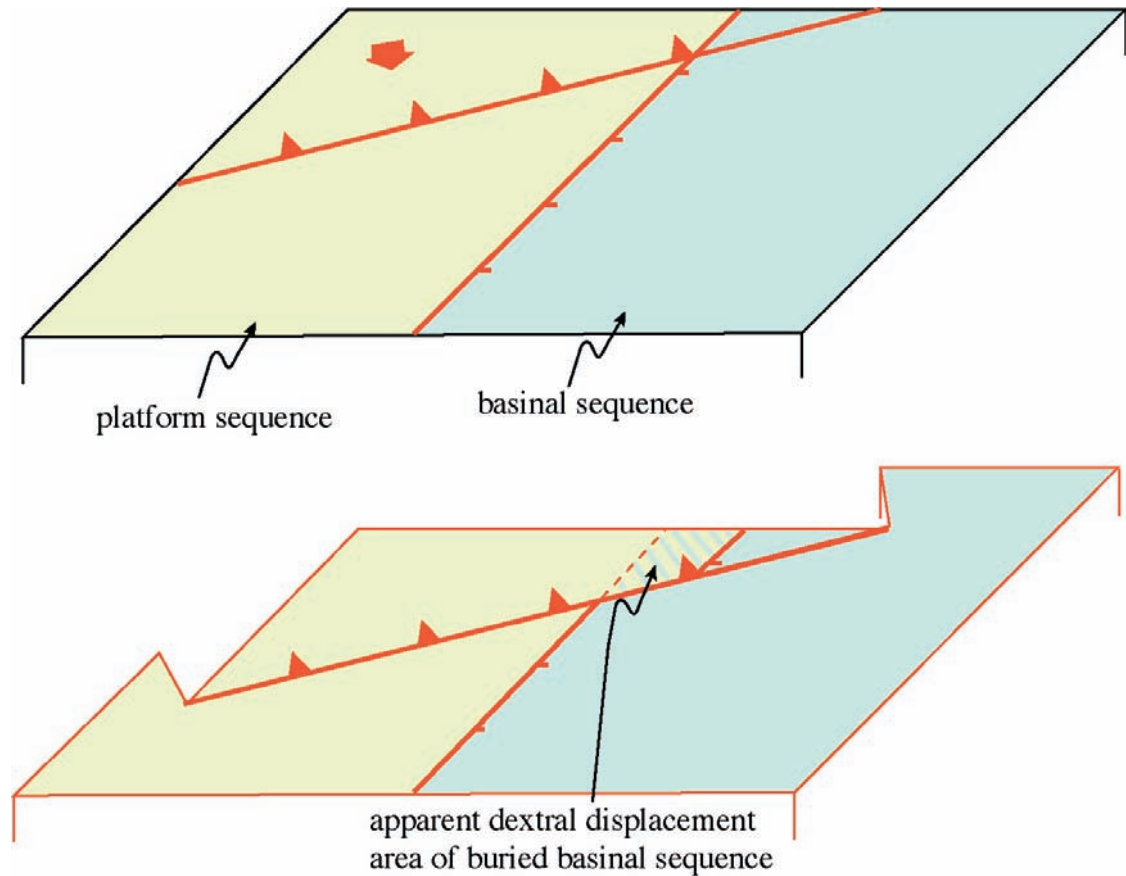


Fig. 162 - A thrust obliquely affecting a platform-basin margin will produce an apparent dextral displacement. For instance the Trento Platform was thrust towards southeast over the Belluno Basin in the Venetian Prealps along the Belluno Thrust, due to the southalpine $N20^{\circ}-30^{\circ}W$ compression oblique to the Mesozoic N-S trending margin.

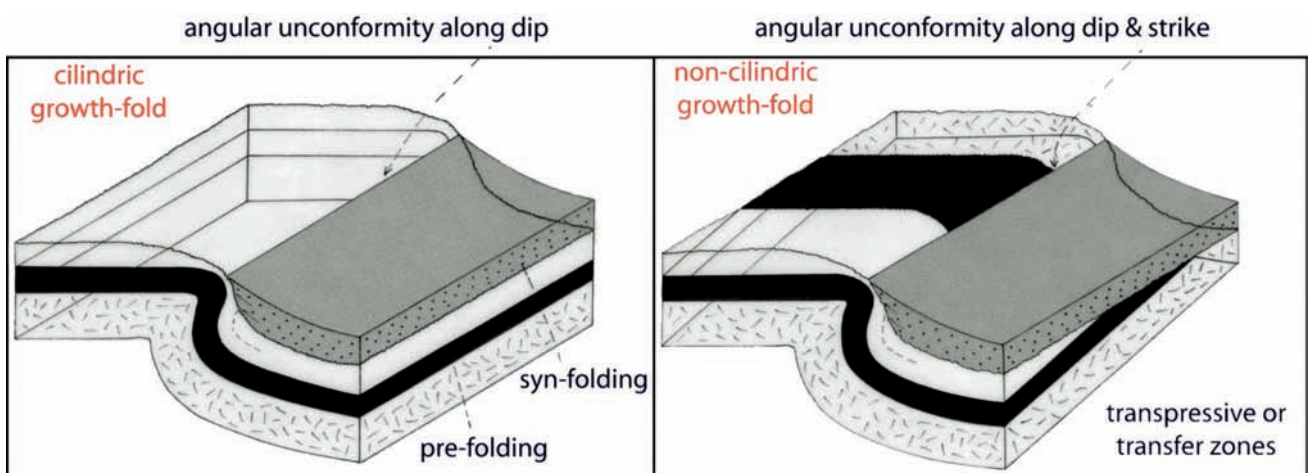


Fig. 163 - The front of the fold-and-thrust belt is characterised by clastic syntectonic deposition. With the progressive growth of the belt, the molassic deposits tend to onlap the flank of the frontal growth anticline. If the frontal anticline is cylindrical, the resulting unconformity will interest only the dip angle. In anticlines characterised by axial undulations, the resulting unconformity will occur both along dip and strike.

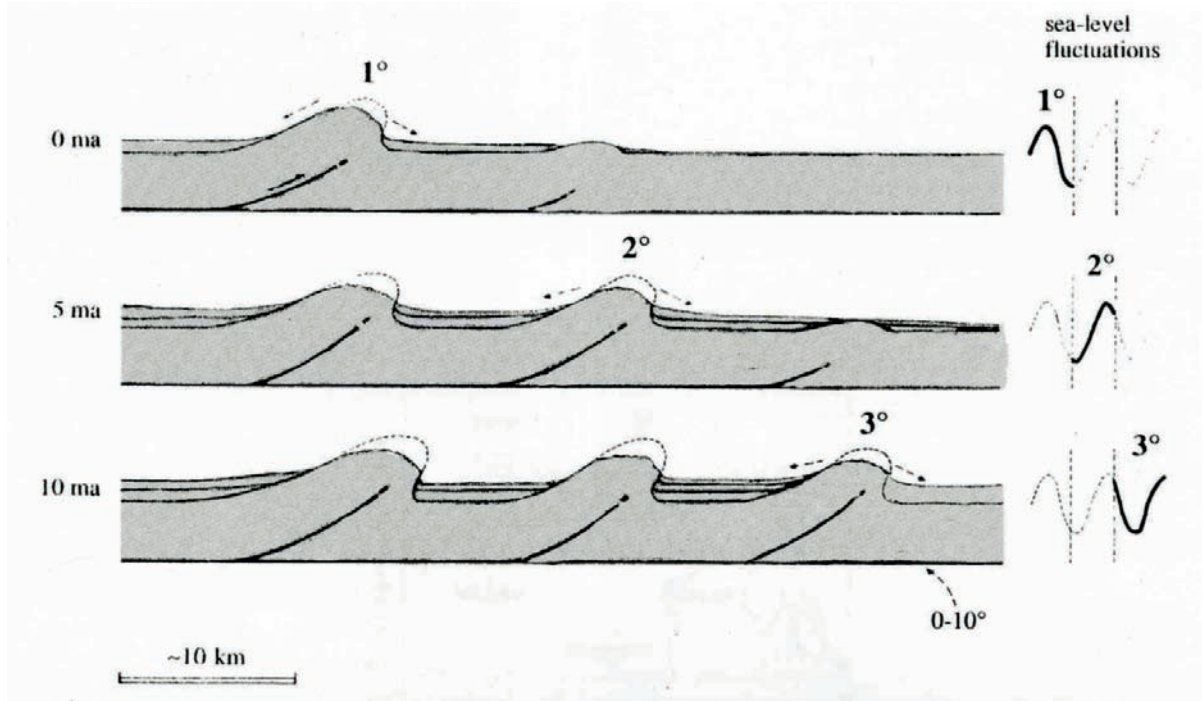


Fig. 164 - Three tectonic cycles may occur during three different segments of a eustatic curve. The depositional sequences may thus be characterised by different interference patterns between tectonics and eustatism. The fault-propagation folds of an accretionary prism produce episodic and localised uplifts of the belt, which migrate regularly towards the foreland together with the foredeep basin and the depositional sequences associated to the growth of any anticline.

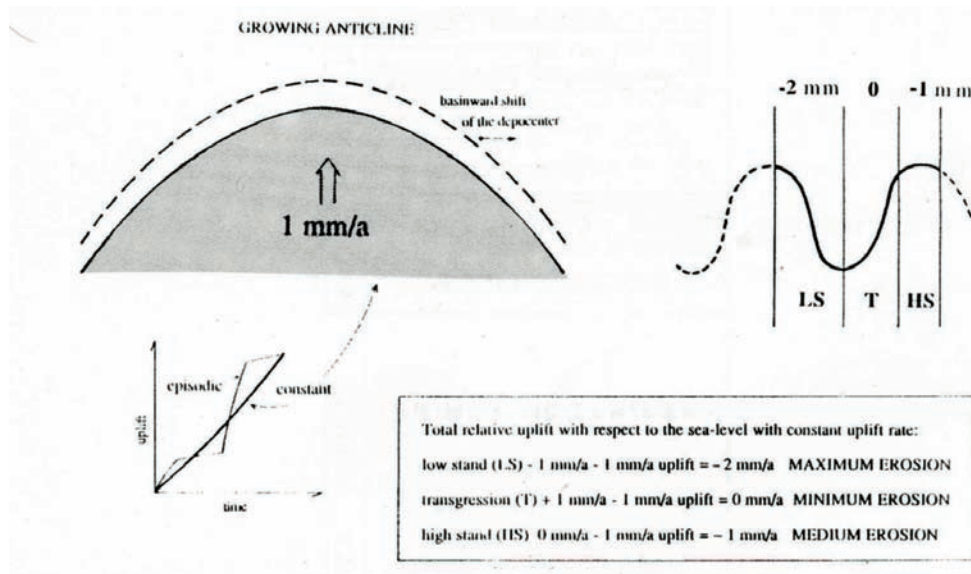


Fig. 165 - The growth of an anticline may be episodic or constant (like the slow steady-state plate motions). In this figure it is shown a scenario characterised by an uplift rate of 1 mm/yr. The uplift is superimposed to a eustatic cycle of third order, represented to the right. During the low stand, with a eustatic sea level fall of 1 mm/yr, the relative sea-level fall at the growing anticline will occur at rates of 2 mm/yr, producing a significant erosion of the anticline. During a transgressional stage with rates of 1 mm/yr, the tectonic uplift will be compensated by the eustatic rise and the relative sea-level will remain constant, inducing minimum rates of erosion of the fold. The assumed uplift and eustatic rates are hypothetical. However, they may help in understanding the problem of the relationship between tectonics and sequence stratigraphy.



Fig. 166 - Panoramic view of platform-to-basin transition at Castiglione (Sabina region, Central Apennines). Notice that the onlapping basinal sediments are at an angle of approximately 20° with respect to the sediments deposited onto the structural high. Such an angle is interpreted as the result of differential compaction affecting basinal sediments in the hangingwall of the paleoescarpment. PCP- pelagic carbonate platforms, (after CARMINATI & SANTANTONIO, 2005).

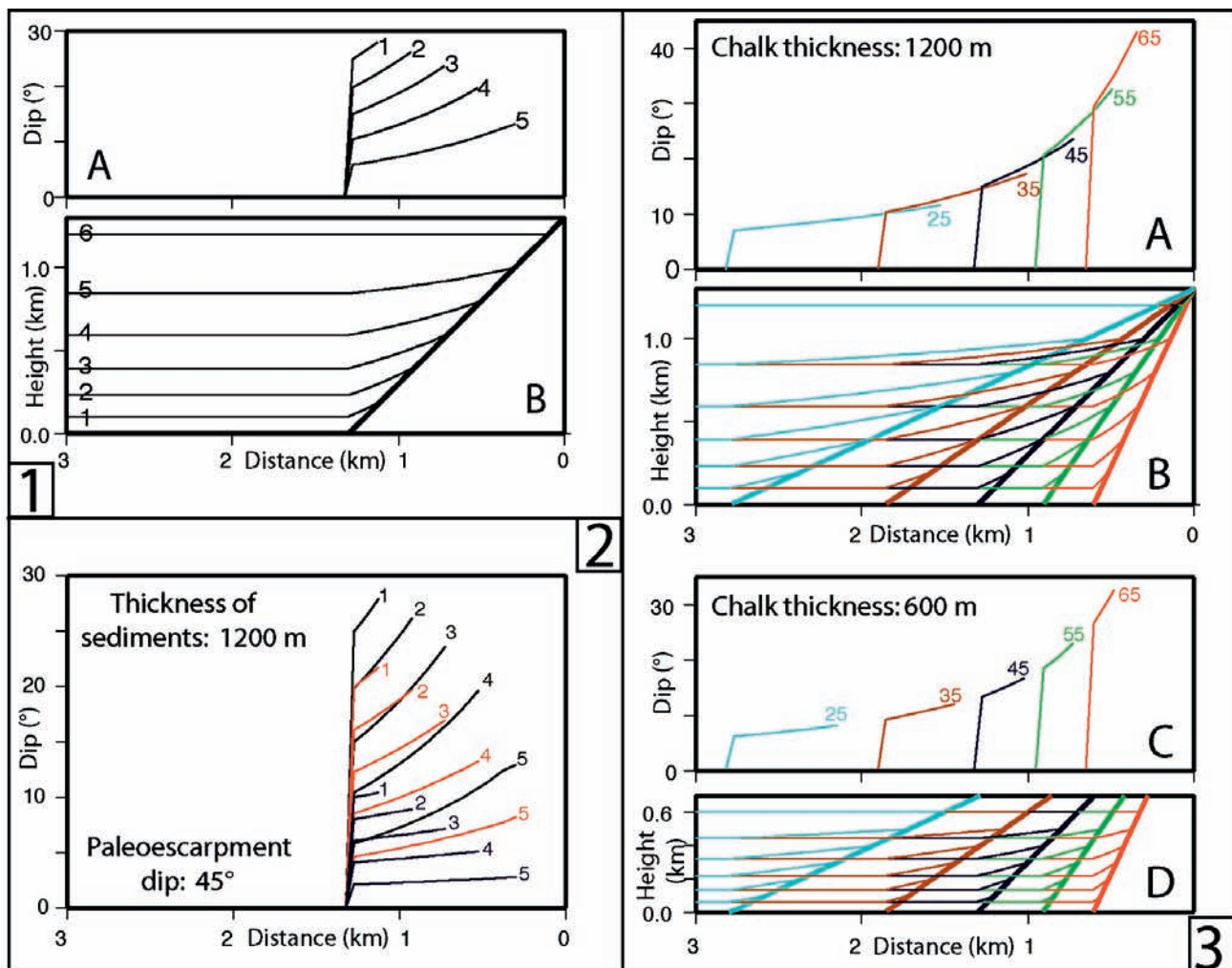


Fig. 167 - This figure shows the results of numerical models of compaction of the basal sediments onlapping a normal fault paleoescarpment. Such results may be, however, extended to sediments onlapping the flanks of anticlines in compressional settings. Notice that the geometry and dip of basal sediments vary consistently with the variation of the sediment nature and of the fault dip. (1) (A) Dip and (B) geometry predicted for a 1200-m-thick succession of chalk onlapping an escarpment dipping 45° . (2) Dip predicted for 1200-m-thick chalk (black), shale (red), and sandstone (blue) successions onlapping an escarpment dipping 45° . (3) (A, C) Dip and (B, D) geometry predicted for chalk section (1200 m and 600 m thick, respectively) onlapping escarpments with dips ranging between 25° and 65° . In A and C, dip is referred to level 3. Colors indicate simulations with different escarpment dips: cyan, 25° ; brown, 35° ; blue, 45° ; green, 55° ; red, 65° (after CARMINATI & SANTANTONIO, 2005).

racterised by more inclined basement monoclines, the internal synclines may be filled by larger volumes of clastic deposits (figs. 168, 169).

Fold uplifts compete during their development with regional subsidence in the frontal parts of thrust belts and accretionary wedges. Two cases exist in frontal thrust belts. In the first, most common case, the uplift rate of the external folds is higher than the subsidence rate of the foredeep. In the second case the fold uplift is less than the regional subsidence. The total fold uplift may be considered as the fold uplift rate minus the regional subsidence rate; this value can be either positive or negative. The positive total fold uplift occurs when folds rise faster than regional subsidence and the envelope of the fold crest rises toward the hinterland of the accretionary wedge. In the opposite case, the negative total fold uplift, the envelope dips toward the hinterland because

folds rise slower than the regional subsidence. In the first positive case the folds are deeply eroded and the onlap of the growing strata moves away from the fold crest if the sedimentation rate is lower than the fold uplift rate in marine or alluvial environments. In the second negative case, where folds rise at lower rates than the regional subsidence, the onlap moves toward the fold crest if the sedimentation rate is higher than the fold uplift rate. This is also the more favorable case for hydrocarbon traps where growth strata can seal the fold. Moreover the fast subsidence rates in the foredeep provide a higher thermal maturation. This second tectonic setting is commonly associated with accretionary wedges forming along west-dipping subduction zones, which are characterized by high subsidence rates in the foredeep or trench, due to the fast "eastward" roll-back of the subduction hinge (e.g. Apennines, Carpathians, Banda arc).

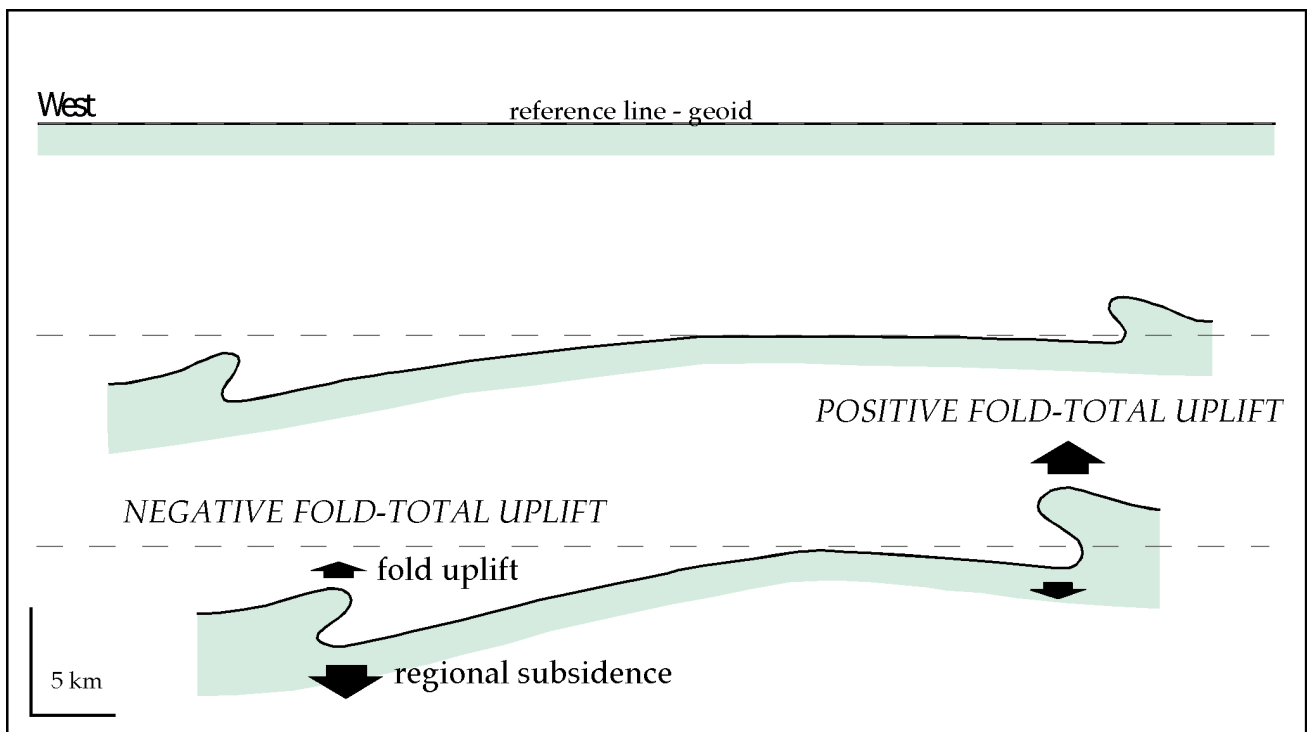


Fig. 168 - The fold-total uplift may be defined as the single fold uplift minus the regional subsidence. This value can be either positive or negative. This last case may occur along the front of W-directed subduction zones where the subsidence rates may be faster than the fold uplift rate.

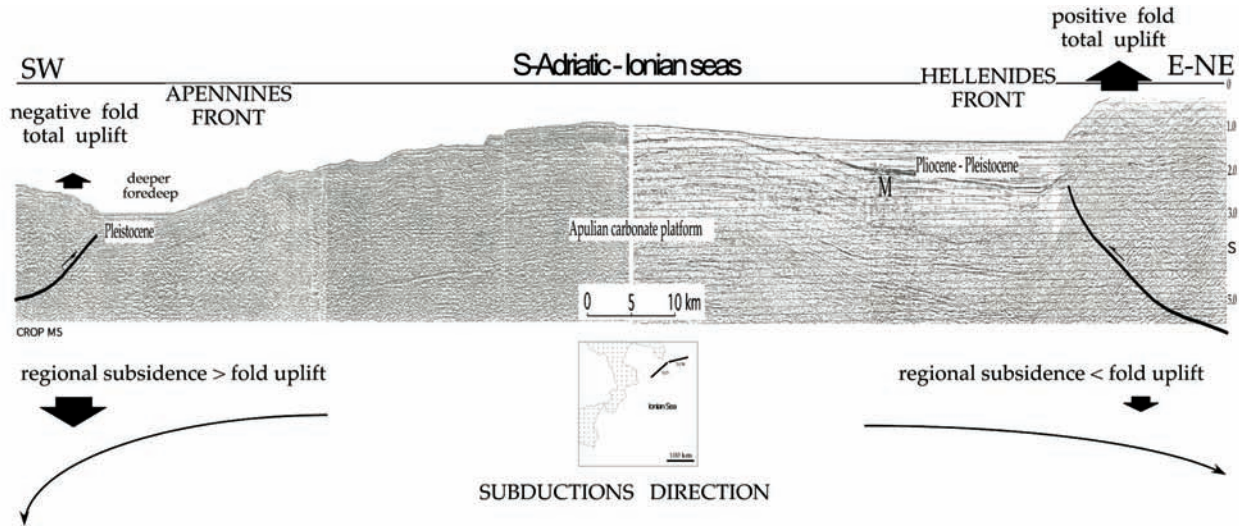


Fig. 169 - Comparison between the Apennines and Dinarides-Hellenides front in the southern Adriatic-Ionian seas. Note the deepest foredeep along the Apennines subduction and the higher structural elevation of the Hellenides front. M, Messinian. The Apenninic front has negative fold-total uplift, whereas in the Hellenides it is positive.

Normal faults occur in a variety of geodynamic environments, both in subsiding and uplifting areas (figs. 170 -174). Normal faults may have slip rates faster or slower than regional subsidence or uplift rates. The total subsidence may be defined as the sum of the hangingwall subsidence generated by the normal fault and the regional subsidence or uplift rate. Positive total subsidence obviously increases the accommodation space (e.g. passive margins

and back-arc basins), in contrast with negative total subsidence (e.g. orogens). Where the hangingwall subsidence rate is faster than the sedimentation rate in case of both positive and negative total subsidence, the facies and thickness of the syntectonic stratigraphic package may vary from the hangingwall to the footwall. A hangingwall subsidence rate slower than sedimentation rate only results in a larger thickness of the strata growing in the hangin-

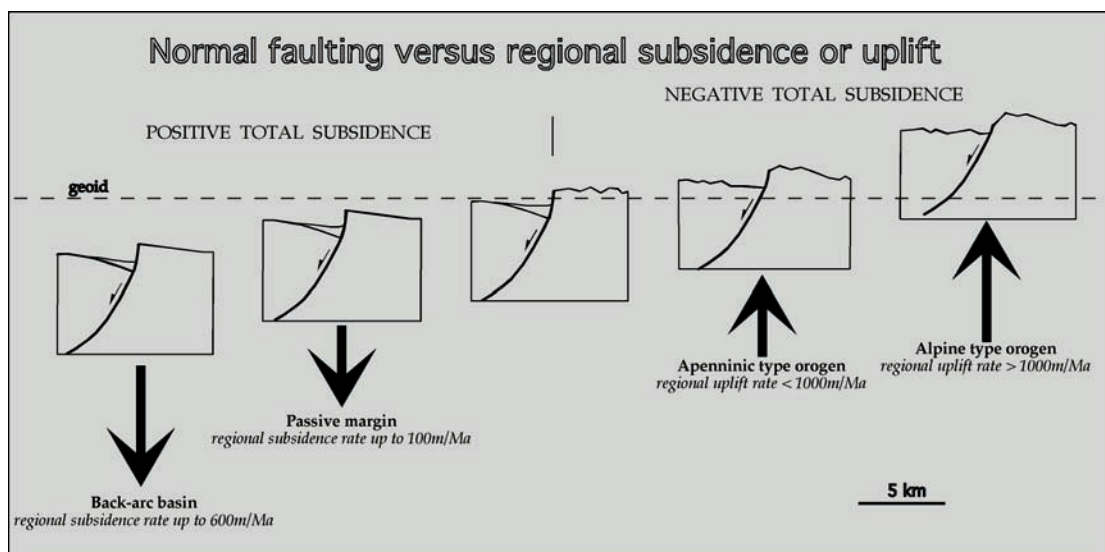


Fig. 170 - Normal faults form in almost all geodynamic settings. The subsidence they generate competes with regional thermal subsidence, lithospheric thinning or uplifting orogens along subduction zones.

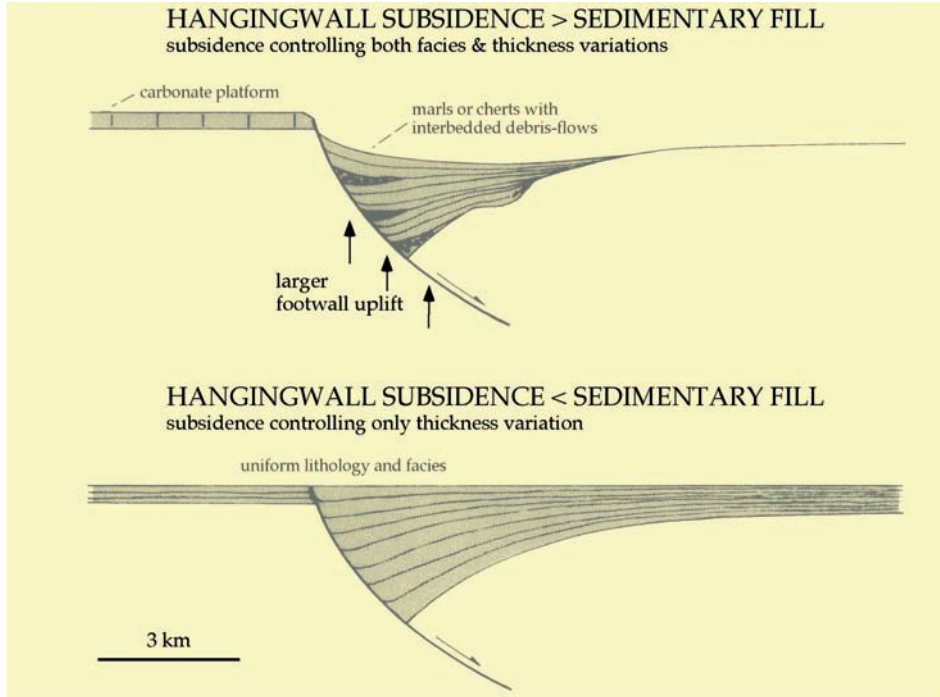


Fig. 171 - Relationship between tectonics and stratigraphy across an extensional syn-sedimentary fault. Subsidence rates and sediment supply are independent factors that have different values in different geodynamic settings. When the subsidence rate along a fault is larger than the sedimentation rate, there is a morphological step at the fault and this may generate lateral facies changes (upper panel). When the subsidence rate is lower than the sedimentation rate, the fault only controls the thickness of the syntectonic sediments and the morphological gradient is absent in any kind of sedimentary environment, e.g., both subaerial and shallow or deep marine facies (lower panel). In the former case, a higher footwall uplift should be expected due to the mass deficit. Interbedded debris flows may be sourced both by the fault scarp and by the limb of the rollover anticline. Debris-flow deposits (megabreccias) of this origin intercalated in a sedimentary successions should not be confused with low-stand wedge deposits generated by global eustatic falls.

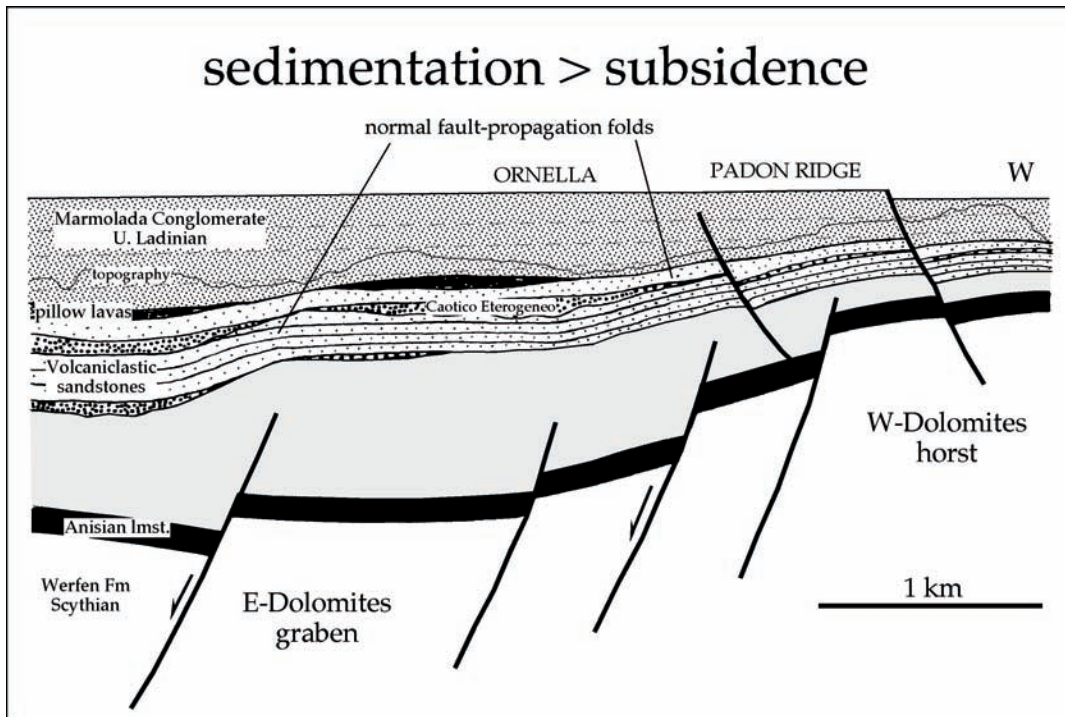


Fig. 172 - Cross-section at the end of the Ladinian along the Padon Massif (Dolomites). Syntectonic N-S trending normal faults formed with subsidence rates slower than sedimentation rate and no facies changes occur across the faults.

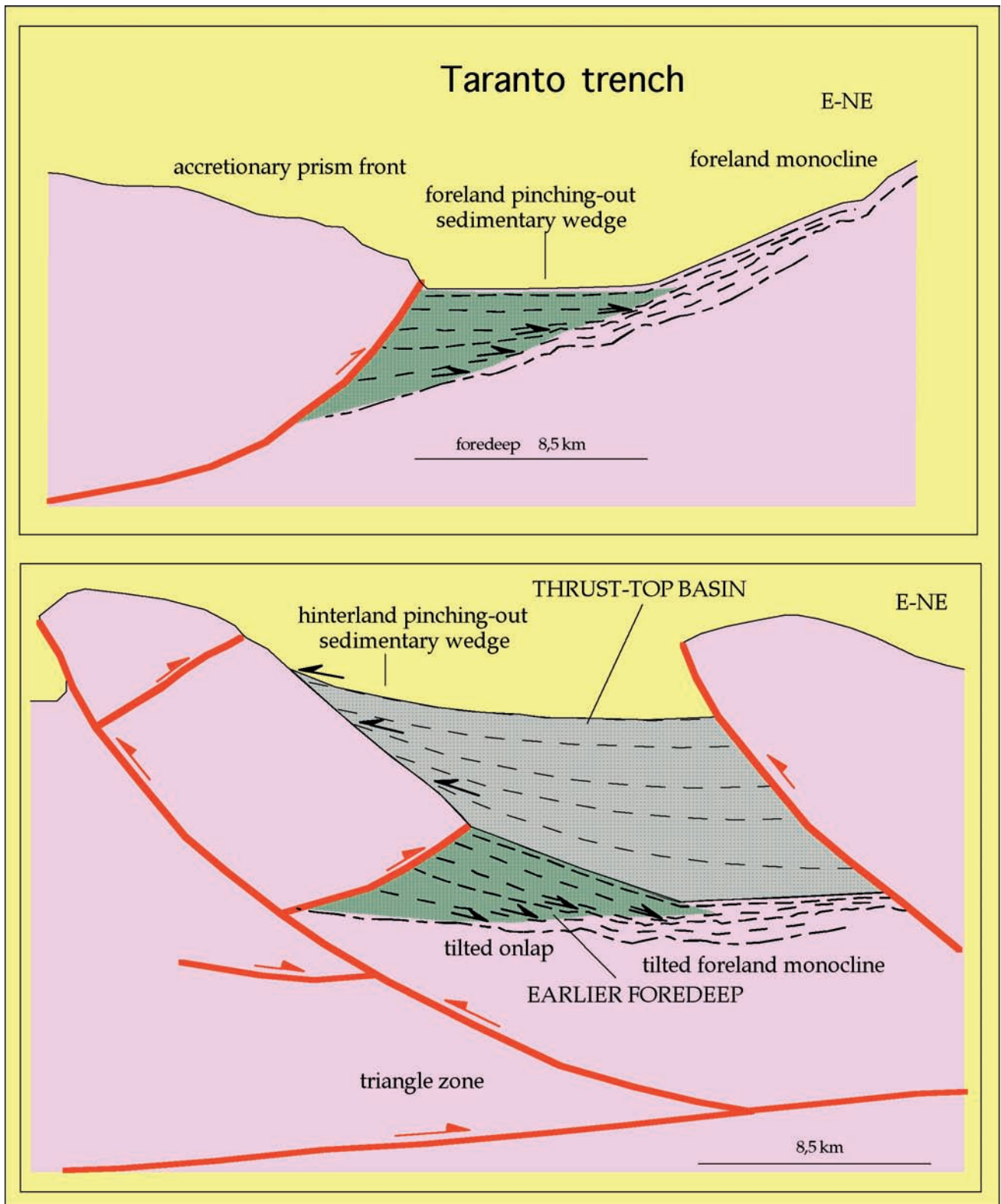


Fig. 173 - Interpretation of the geometric structural and stratigraphic pattern at the front and within the Apennines accretionary prism in the Ionian Sea. The present front (above) could represent the early foredeep stage later tilted by backthrusting (below). The original onlap onto the foreland regional monocline, and pinching-out of the sedimentary packages, once tilted, mimics an apparent downlap in the internal section below. The shape and width of the basin is controlled by ramp distances and vergences.



Fig. 174 - Example of the Apennines history. Pizzo Intermesoli, Gran Sasso Range, central Apennines. Jurassic transtensional tectonics sealed by Cretaceous basinal facies are preserved in a thrust sheet presently cross-cut by active normal faults to the left. Active thrusting is presently displaced eastward in the Adriatic coast.

gwall, with no facies changes and no morphological step at the surface. The isostatic footwall uplift is also proportional to the amount and density of the sediments filling the half-graben and therefore it should be more significant when the hangingwall subsidence rate is higher than sedimentation rate.

The foreland monocline dips underneath thrust belts and accretionary wedges, both in oceanic and continental subduction zones (fig. 175). Figure 176 shows the dip of the monocline in the frontal part of two orogens, the Alps and the Apennines. There is an overall difference between the dip of the relative monoclines, and there is also a strong lateral variation along both arcs. In the Alps, the regional dip varies between 0° in the remote foreland, to an average of $2-3^\circ$ at the front of the thrust belt below the foredeep, to about 5° beneath the external thrust-sheets within 40 km from the leading edge of the accretionary wedge. The regional dip of the monocline in the

Apennines has an average of $4-5^\circ$ at the front of the thrust belt below the foredeep, to about 10° beneath the external thrust-sheets within 40 km from the leading edge of the accretionary wedge. There are areas where the dip exceeds 20° .

The Apennines though topographically lower than the Alps present higher monocline dips and a deeper foredeep. Moreover, there are variations in the dip of the monocline moving along strike of the two belts: the low values coincide with Permian-Mesozoic inherited horsts, whereas the steeper values correspond to basinal areas, and they usually match the salients of the thrust belt front. Within the salients the distance between thrust ramps increases.

Therefore there are two orders of mean values of the dip of the foreland monocline, the first at the orogen scale (more than 1000 km wavelength), the second at the regional scale (100-200 km wavelength) within the single orogen.

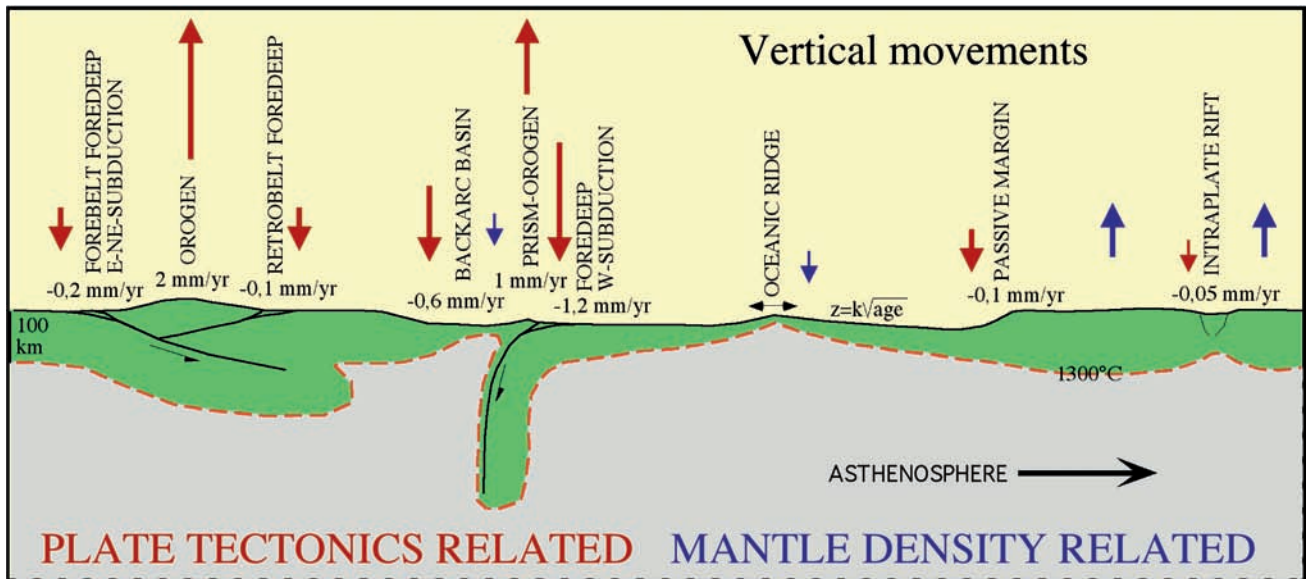


Fig. 175 - Mean vertical movements along the main geodynamic settings, i.e., foredeeps, passive continental margins, and rifts. Foredeeps subside for the flexure of the lithosphere generated by the loading of the upper plate along E- to NE-directed subduction zones, whereas they are possibly generated by the flexure generated by the opposite mantle flow along W-directed subduction zones. Oceanic embayments are subsiding mostly for the cooling and thickening of the lithosphere, where z is the depth of the ocean floor relative to the ridge, and K is a constant (320). Backarc rifts, passive margins and intraplate rifts are generated primarily by thinning of the lithosphere, plus thermal and loading effects. The red dashed line indicates the inferred trend of the isotherm marking the lithosphere base.

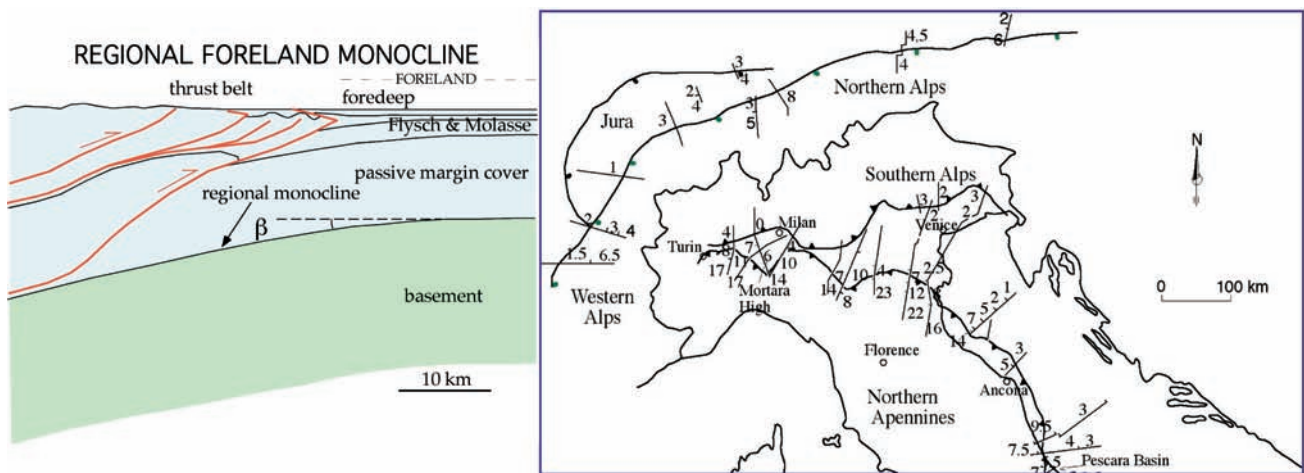


Fig. 176 - The dip of the regional foreland monocline is a significant signature of thrust belts. In spite of the higher elevation, the Alps have in average lower dip of the monocline with respect to the Apennines. This asymmetry might be ascribed to the different polarity of the subduction (after MARIOTTI & DOGLIONI, 2000).

Lateral variations in the lithospheric buoyancy due to the inherited Mesozoic stretching may explain the second order variations in foreland dip, but not the first order mean values which seem to be more sensitive to the geographic polarity of the subduction rather than to the lithospheric composition which is

rather similar in the Alpine and in the central-northern Apennines slabs.

The geological characteristics of foredeeps and accretionary wedges suggest that these features are distinguishable on the basis of the direction of the associated subduction (figs. 177 - 179). East- northeast-dipping subduction-related

accretionary wedges show high relief and broad outcrops of metamorphic rocks. They are associated with shallow foredeeps with low subsidence rates. In contrast west-dipping subduction-related accretionary wedges show low relief and involve mainly sedimentary cover. The related foredeeps are deep and have high subsidence rates (figs. 180, 181). This differentiation is useful both for oceanic and continental subductions, e.g., eastern vs. western Pacific subductions, or east-dipping Alpine vs. west-dipping Apenninic subductions (figs. 182, 183, 185). In a cross-section of the Alps the ratio of the area of the orogen to the area of the foredeeps is at least 2:1, whereas this ratio is 0.22:1 for the Apennines. These ratios explain why foredeeps related to east- or northeast-dipping subduction are quickly filled

and bypassed by clastic supply, whereas foredeeps related to west-dipping subduction maintain longer deep water environment. These differences support the presence of an "eastward" asthenospheric counterflow relative to the "westward" drift of the lithosphere detected in the hot-spot reference frame, even in the Mediterranean where no hot spots are present (fig. 184). In this interpretation, the Apennines foredeep was caused by the "eastward" push of the mantle acting on the subducted slab, whereas the foredeeps in the Alps were caused by the load of the thrust sheets and the downward component of movement of the upper Adriatic plate; these forces contrast with the upward component of the "eastward" mantle flow.

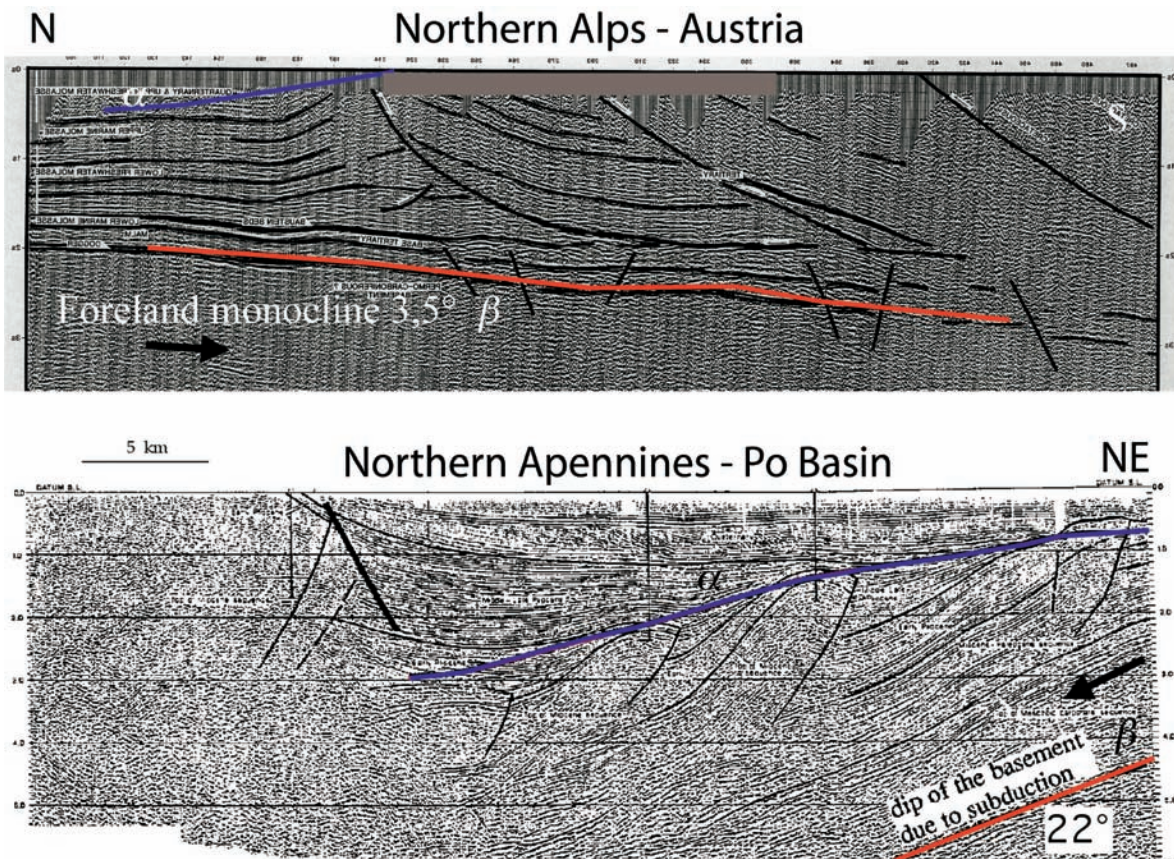


Fig. 177 - Two examples of the regional foreland monocline dip in red (β) from the Alps, above, and the Apennines, below. The envelope of the fold crests in blue (α) rises toward the interior of the belt in the Alps, whereas it may dip toward the interior of the prism in the Apennines. This last geometry occurs if the regional subsidence is faster than the fold uplift. Seismic sections after BACHMANN & KOCH (1983) and PIERI (1983).

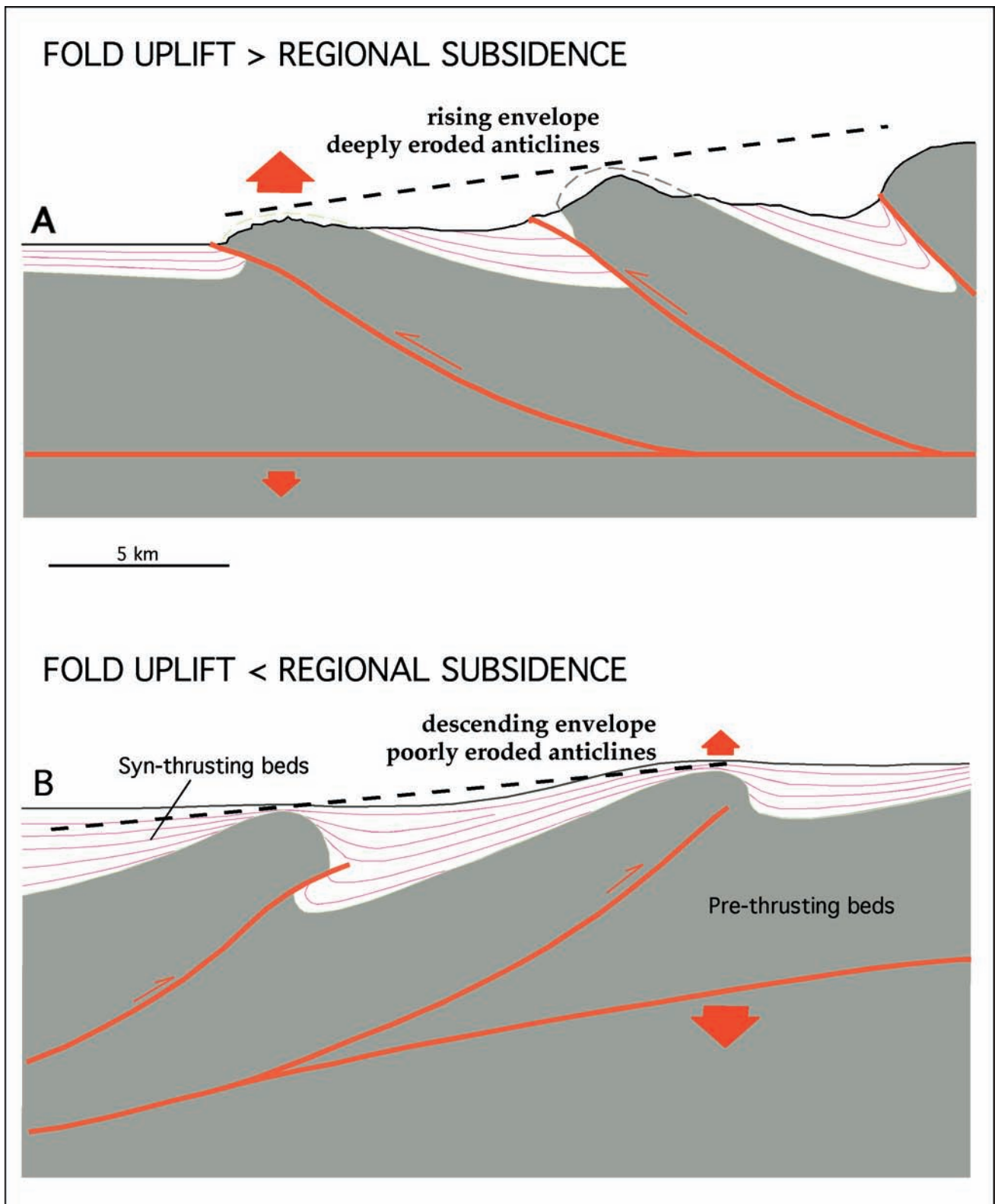


Fig. 178 - Fold uplift rates may be higher or lower than the regional subsidence of the foredeeps. In the classic case A, the envelope of the fold crests is rising toward the hinterland, and the anticlines are deeply eroded. In the case B the fold uplift rate is lower than the regional subsidence rate, as a result of which, the envelope to the fold crests descends toward the hinterland and the anticlines are not significantly eroded (after DOGLIONI & PROSSER, 1997).

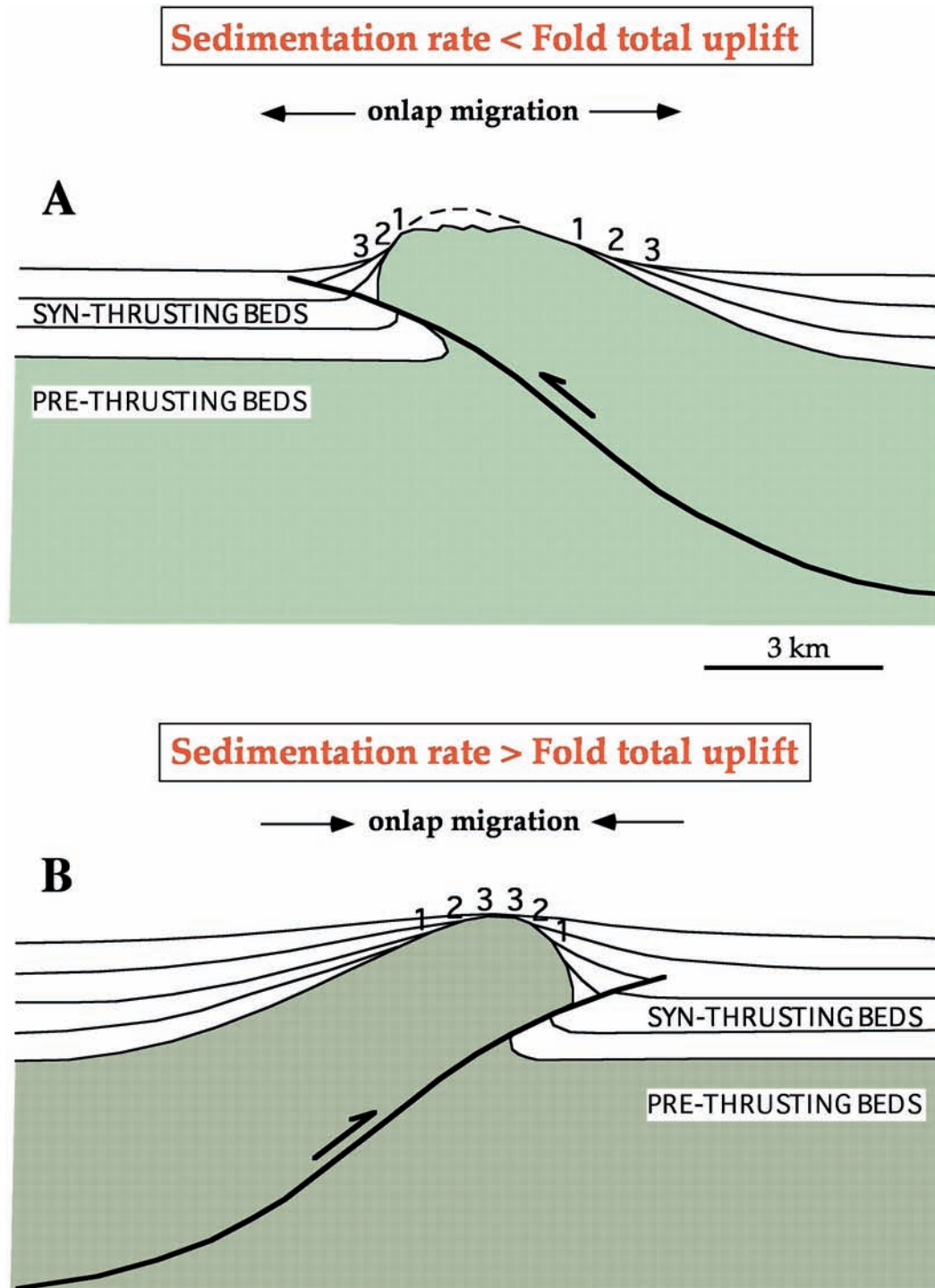


Fig. 179 - Where the fold uplift rate is greater than regional subsidence rate, the onlaps of the syntectonic beds move away from the fold crest, and the sedimentation rate is lower than the fold total uplift (A). On the other hand, onlaps may migrate toward the fold crest where the fold uplift rate is less than the regional subsidence rate, and the sedimentation rate is higher than the fold total uplift (B). The two end members may alternate on the limbs of a fold when for instance in B the fold uplift is lower than the regional subsidence, but the sea-level drops at higher rates exposing the fold.

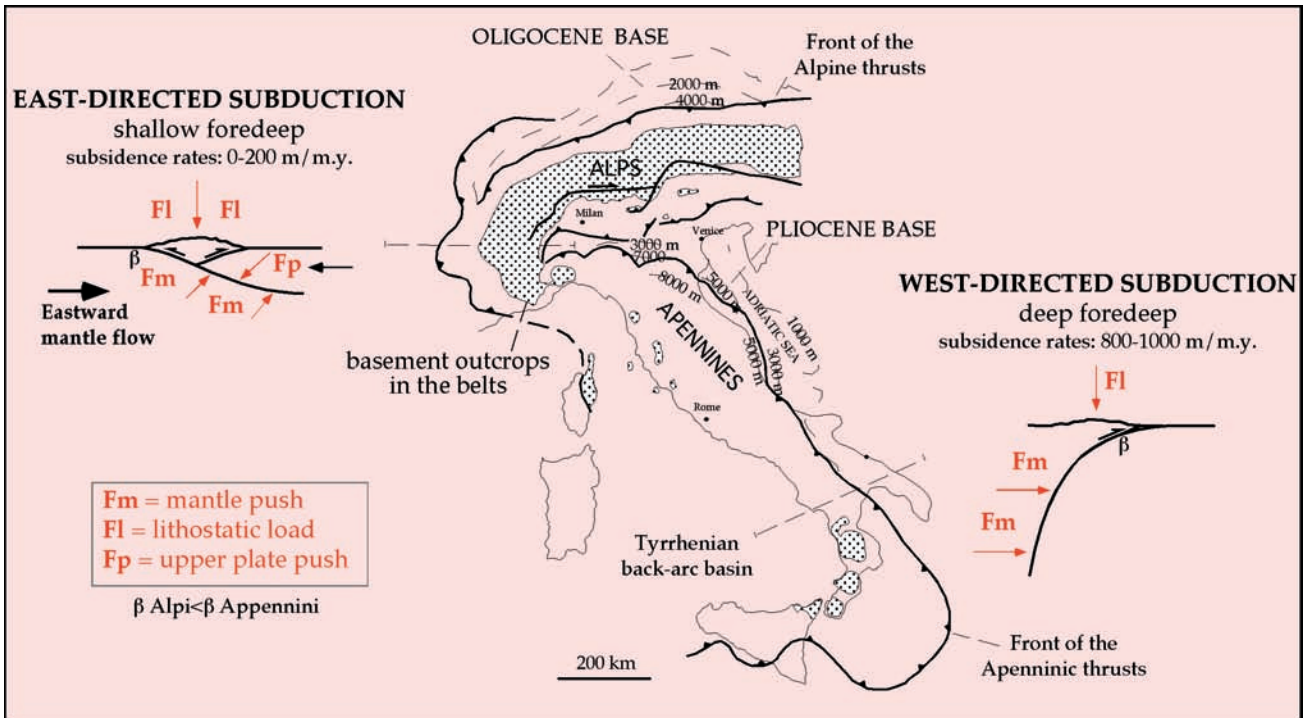


Fig. 180 - Alps and Apennines are thrust belts with very different characters. The Alps have a shallow foredeep, broad outcrops of metamorphic rocks, and high structural and morphologic relief. The Apennines have deep foredeep, few outcrops of basement rocks (partly inherited from earlier Alpine phase), low structural and morphologic elevation, and the Tyrrhenian back-arc basin. These differences mimic asymmetries of Pacific east-directed Chilean and west-directed Marianas subductions. For E-NE-directed subduction foredeep and trench, the origin may be interpreted as controlled by the lithostatic load and the downward component of upper plate push, minus the upward component of the "eastward" mantle flow (upper left panel). For the W-directed subduction where subsidence rate is much higher, the foredeep origin may rather be interpreted as due to the horizontal mantle push and the lithostatic load, panel in the lower right (after DOGLIONI, 1994).

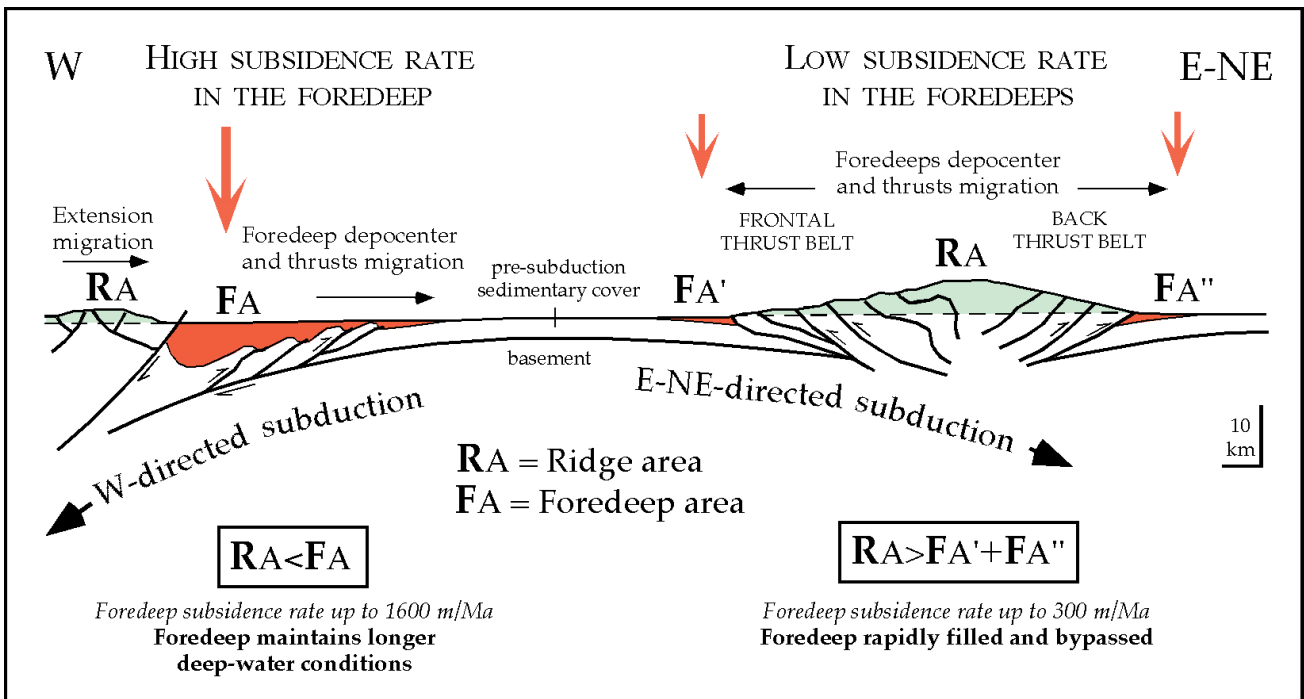


Fig. 181 - Strong asymmetry of the geologic parameters is observed between foredeeps related to west-directed subduction (left), and foredeeps related to east-northeast-directed subduction (right). In the west-directed case, the area of foredeep (filled or unfilled) is wider than the area of mountainous ridge, whereas foredeeps areas are smaller in opposite directed subductions (after DOGLIONI, 1994).

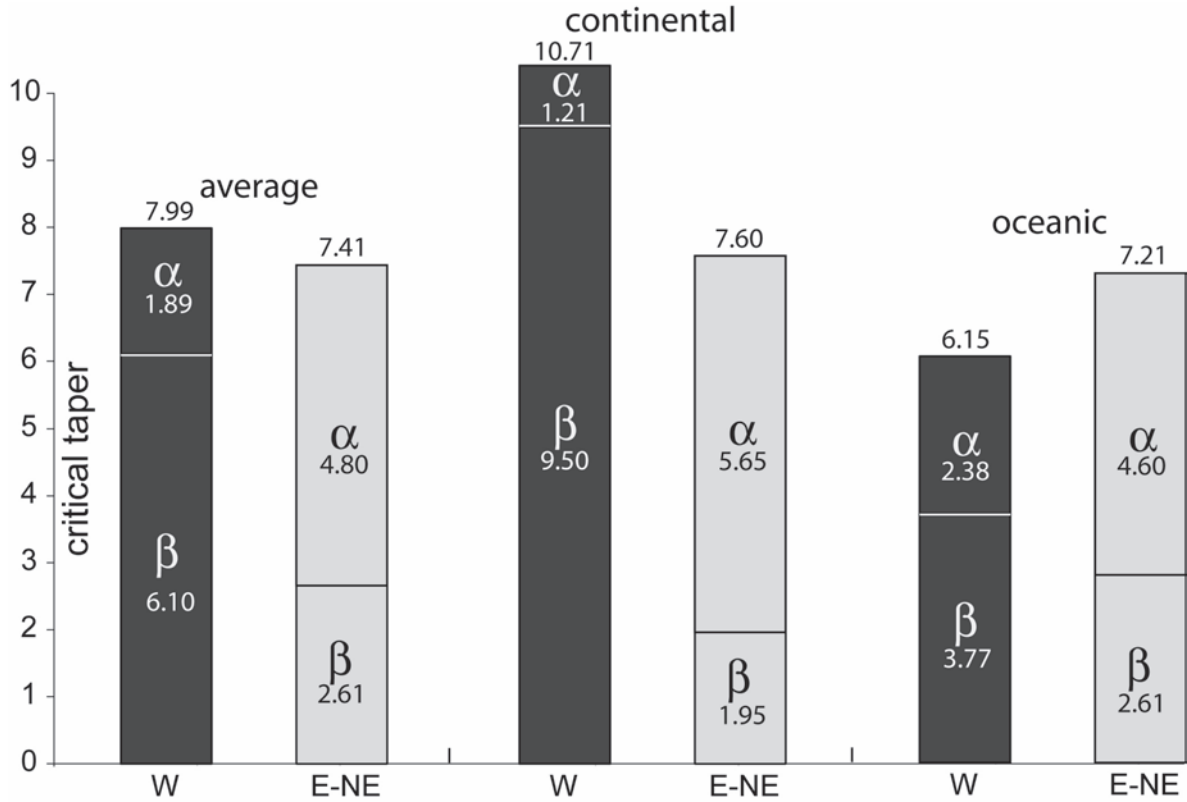


Fig. 182 - Average values of the topographic envelope (α), dip of the foreland monocline (β), and critical taper ($=\alpha + \beta$) for the two classes of subduction zones, i.e., W-directed and E- or NE-directed. Note that the "western" classes show lower values of α and steeper values of β (after LENCI & DOGLIONI, 2007).

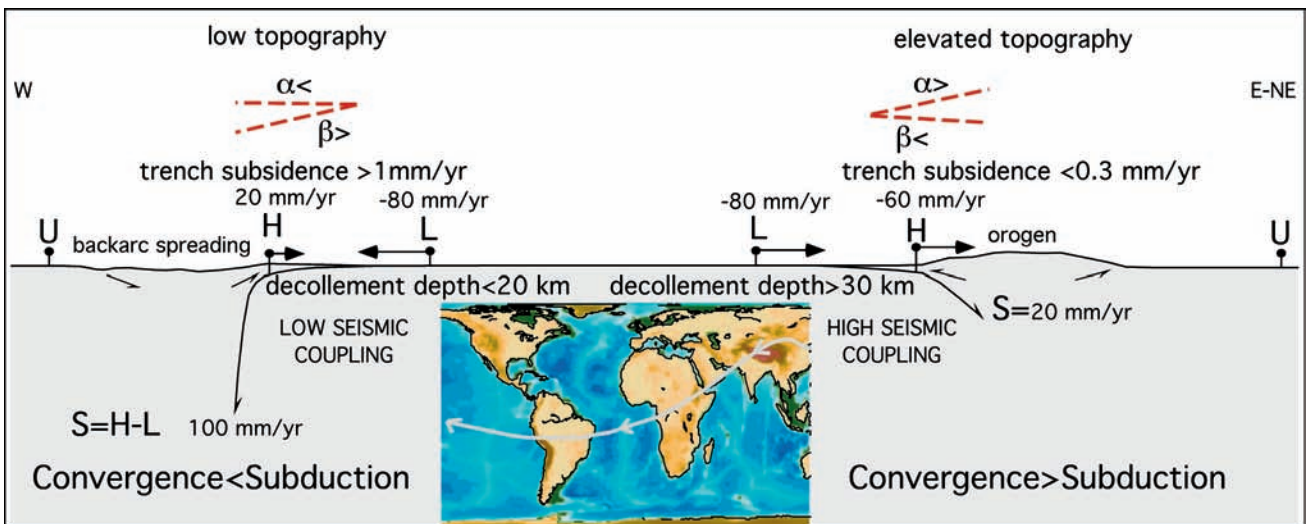


Fig. 183 - Assuming fixed the upper plate U, along west-directed subduction zones the subduction hinge H frequently diverges relative to U, whereas it converges along the opposite subduction zones. L, lower plate. Note that the subduction S is larger than the convergence along W-directed slabs, whereas S is smaller in the opposite case. The two end-members of hinge behavior are respectively accompanied in average by low and high topography, steep and shallow foreland monocline, fast and slower subsidence rates in the trench or foreland basin, single vs. double verging orogens, etc., highlighting a worldwide subduction asymmetry along the flow lines of plate motions indicated in the inset (after DOGLIONI *et alii*, 2007).

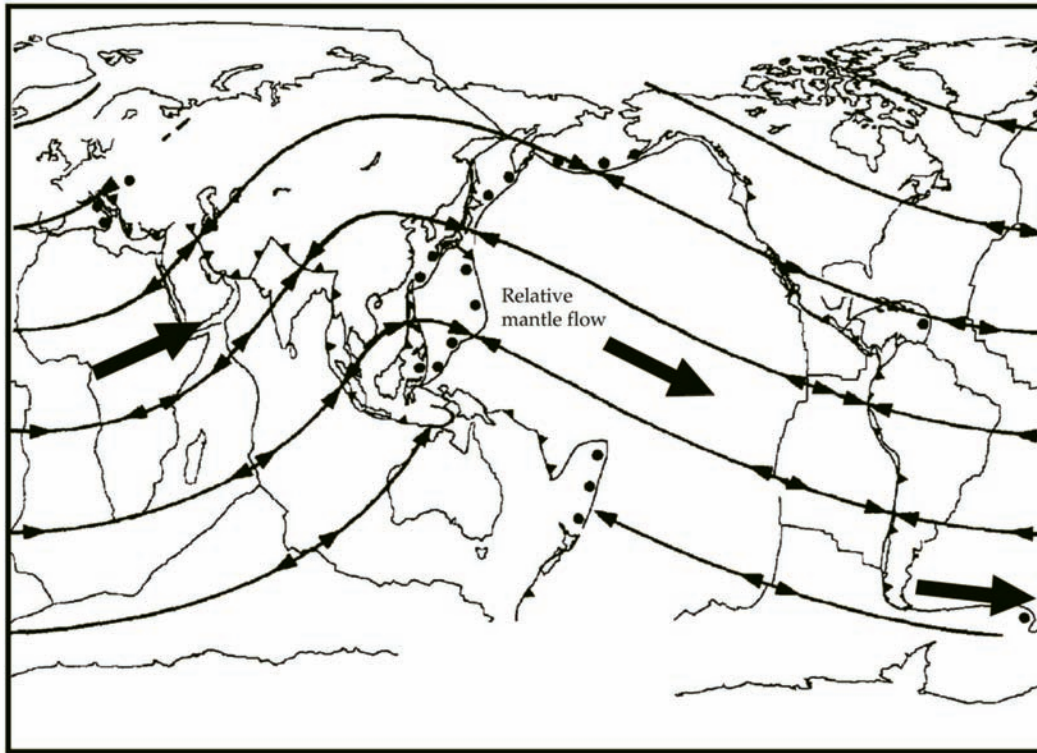


Fig. 184 - Tectonic undulated mainstream along which plates move with a few cm/yr "westward" delay relative to the underlying mantle.

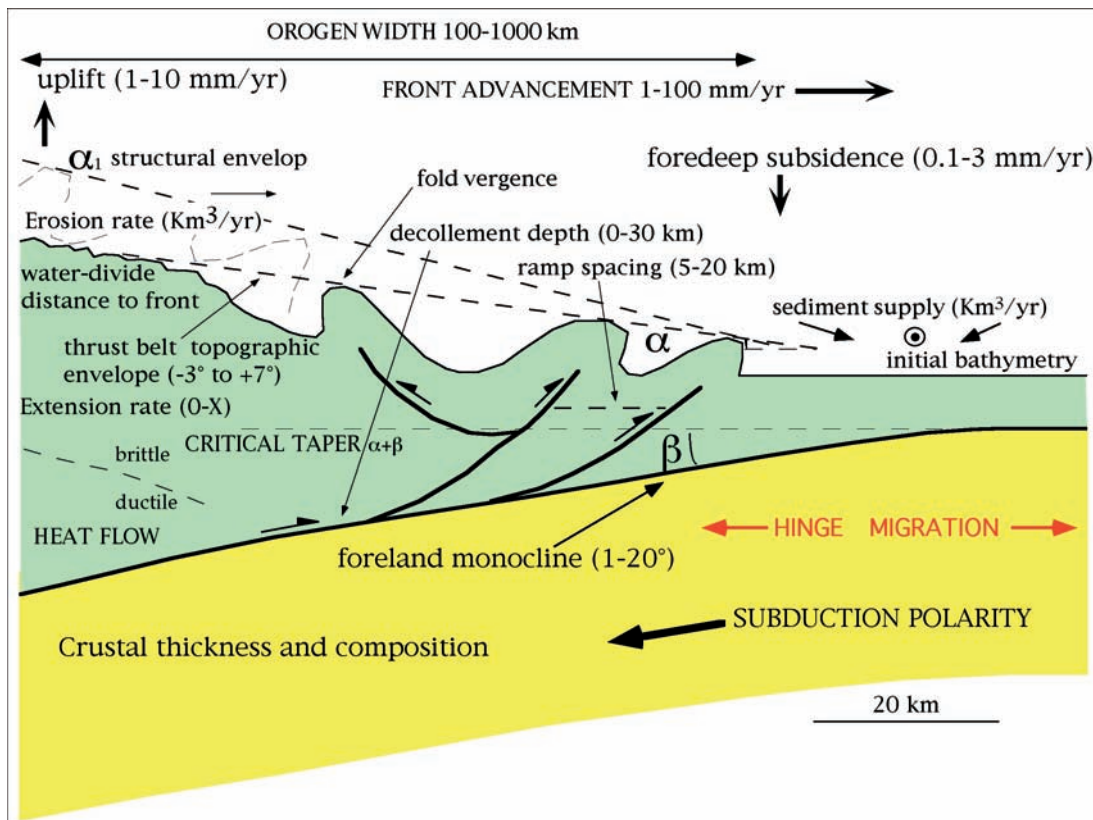


Fig. 185 - The orogens are structured by the combination of a number of parameters. The most important are listed in the figure (after LENCI & DOGLIONI, 2007).

